

LS Scienza dei Materiali - a.a. 2006/07

## Fisica delle Nanotecnologie – part 2

Version 5, Oct 2006

Francesco Fuso, tel 0502214305, 0502214293 - fuso@df.unipi.it  
<http://www.df.unipi.it/~fuso/dida>

# **Tecnologie convenzionali nell'approccio top-down; I: crescita di materiali e strati sottili**

13/10/2006 – 14.30-16.30 – room T1

## Introduction to the topic

Conventional fabrication methods in microelectronics rely on **top-down** approaches, consisting typically of:

- thin film deposition** (typically, alternate layers with different properties);
- Definition of a lateral pattern (**lithography**);
- Selective material removal (**etching**) (or **doping**, or other modifications)

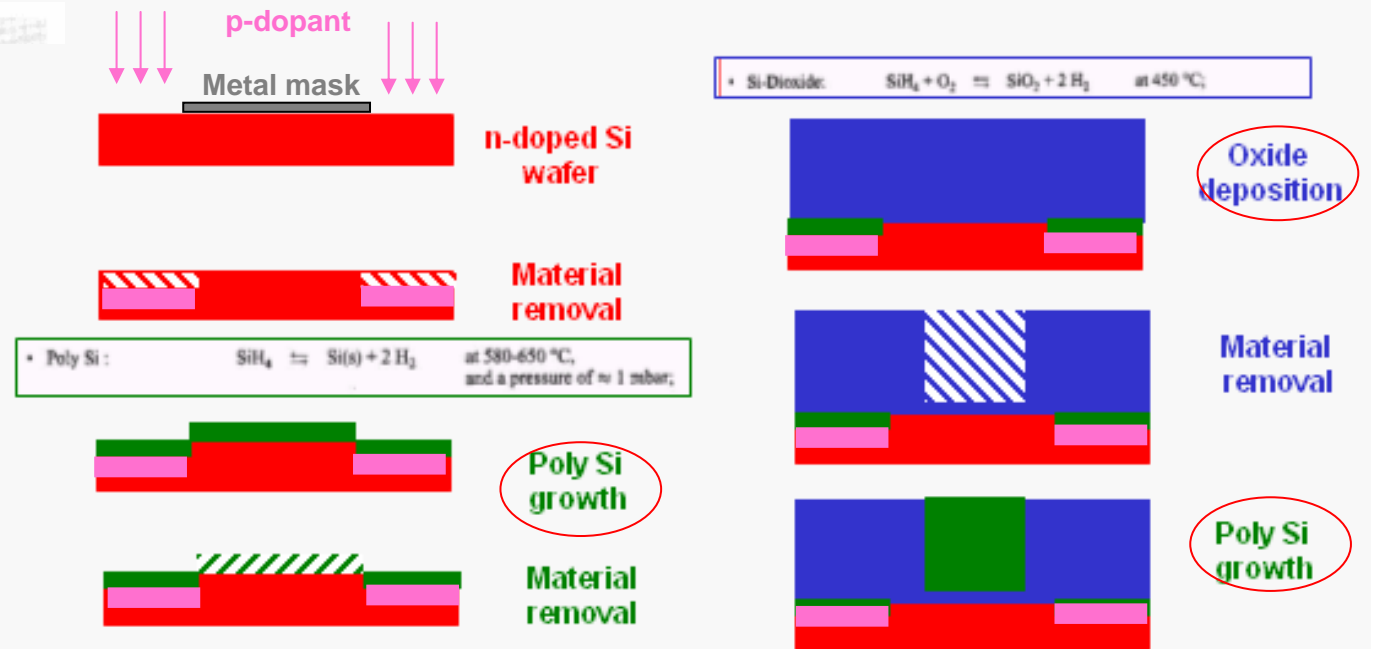
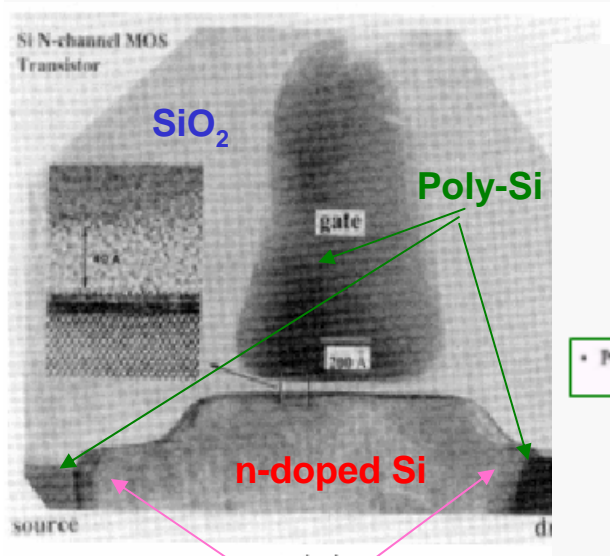
*Frequently, the process is cycled until the final (complex) structure is produced*

Transition from micro- to nano-electronics is somehow hampered by technical and fundamental limitations inherent to the methods

**Where do such limitations come from?**

**We will try to answer this question looking at the different steps involved in the top-down approach  
(we will not mention here organic films)**

# A simple and rough example of multiple technologies



+ other steps (interconnects, passivation, ...)

**A miniaturized MOS-FET**

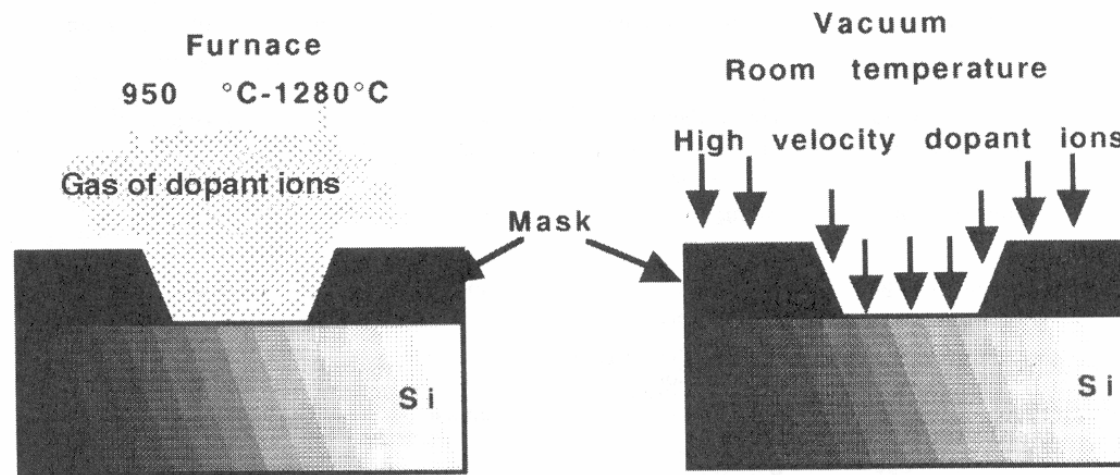
**A possible recipe for fabrication  
(lift-off processes not included)**

Film growth is a basic ingredient: either (poly)crystalline or amorphous materials must be deposited or grown, but in any case high homogeneity and thickness control is desirable; materials of different natures must be deposited, including, for instance, semiconductors, metals, oxides (and also molecular crystal, i.e., organics)

## Example: conventional doping techniques

Inter-crystal diffusion from vapor at high temperature

Ion bombardment at room temperature



**Much more used, now!**

Dopant uniformity and reproducibility	±5% on wafer, ±15% overall	±1% overall
Contamination danger	High	Low
Delineation	Refractory insulators and refractory metals, polysilicon	Refractory and nonrefractory materials, met
Environment	Furnace	Vacuum
Temperature	High	Low

**Si-doping is a highly common technique which requires a mask for lateral definition (a good example to start facing technological problems)**

# A few words on ion implantation

## Ion Implantation

The principle method of doping today centers on high energy ion implantation. Implantation offers the advantage of being able to place any ion at any depth in the sample, independent of the thermodynamics of diffusion and problems with solid solubility and precipitation. Ion beams produce crystal damage that can reduce electrical conductivity, but most of this damage can be eliminated by annealing at 700 to 1000°C.

A beam of energetic ions 'implants' dopants into the substrate. Depth and dopant concentration are controlled by the acceleration energy and the beam current. The stopping mechanism of the ions involves nuclear collisions at low energy and electronic interactions at high energy.

The jargon associated with ion implantation includes:<sup>25</sup>

- Projected range  $R_p$ , i.e., average distance traveled by ions parallel to the beam
- Projected straggle,  $\Delta R_p$ , i.e., fluctuation in the projected range

**Dopant control at the atomic scale can be hardly achieved by conventional doping methods**

## Problems in space definition

- Lateral straggle,  $\Delta R_p$ , i.e., fluctuation in the final rest position, perpendicular to the beam
- Peak concentration,  $N_p$ , i.e., concentration of implanted ions at  $R_p$

The concentration profile, to a first order approximation, is Gaussian, i.e.,

$$N(x) = N_p \exp \left[ -\frac{(x - R_p)^2}{2(\Delta R_p)^2} \right] \quad 3.61$$

$$N_p = \frac{Q}{\sqrt{2\pi\Delta R_p}}$$

The range is determined by the acceleration energy, the ion mass, and the stopping power of the material. Orientation of the substrate surface away from perpendicular to the beam prevents channeling which can occur along crystal planes, ensuring reproducibility of  $R_p$ . Ion-channeling leads to an exponential tail in the concentration vs. depth profile. This tail is due to the crystal lattice and is not observed in an amorphous material. The dose is determined by the charge per ion,  $zq$ ; the implanted area,  $A$ ; and the charge per unit time (current) arriving at the substrate. In other words:

$$\int i dt = Q \quad \text{and} \quad \frac{Q}{|zqA|} = \text{Dose (atoms/cm}^2\text{)} \quad 3.62$$

The technique is now commonly used with penetration depths in silicon of As, P, and B typically being 0.5, 1, and 2  $\mu\text{m}$  at 1000 kEV.

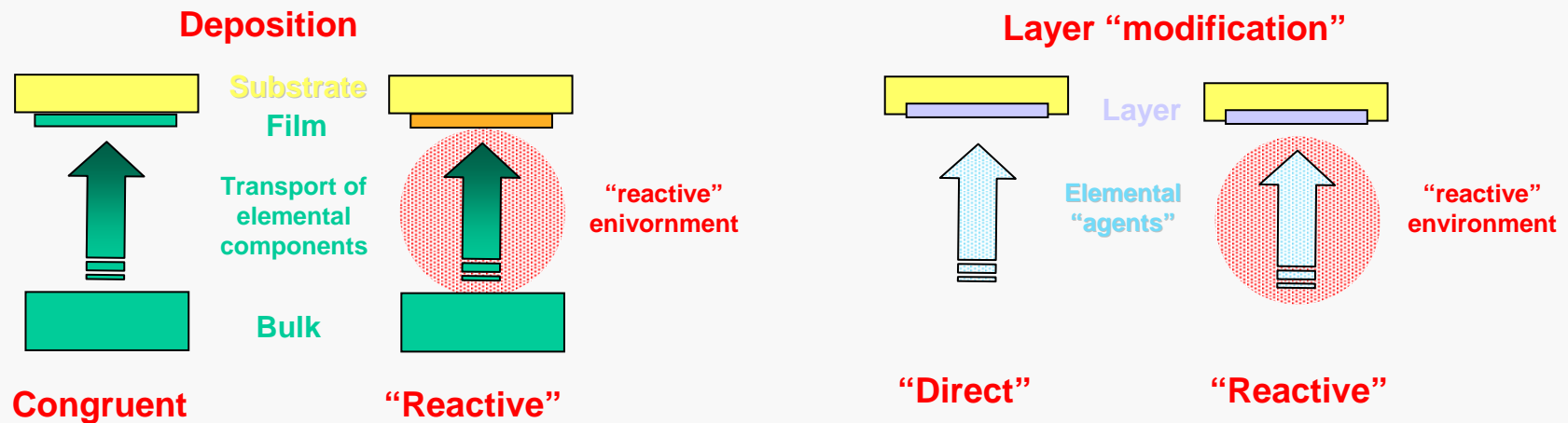
Thermal annealing at temperatures above 900°C is required to remove damage to the silicon lattice and to activate the implanted impurities. For deep diffusions ( $>1 \mu\text{m}$ ), implantation is used to create a dose of dopants, and thermal diffusion (limited source) is used to drive in the dopant.

Ion beams can implant enough material to actually form new materials, e.g., oxides and nitrides, some of which show improved wear and strength characteristics.

# Requirements to be met when miniaturization is concerned

Any fabrication step must aim at:

- precise dimensional control at the nano level (thickness, in case of films);
- *homogeneity and defect-free* materials at the atomic/molecular level



Fabrication of layers typically involve a passage through the "elemental" stage:

- a bulk is dissociated into elements (vapor or liquid) which are re-collected onto a substrate (deposition, i.e., "miniaturization by evaporation, according to Feynman);
- elemental components are used to modify (mostly, chemically) a layer (at the surface or in the depth, as for doping)

## Outlook

1. Basic mechanisms ruling film growth (epitaxy)
2. Basic surface phenomena involved in film growth (diffusion, nucleation, coalescence)
3. Some “physical” deposition methods:
  - A. Molecular beam epitaxy (MBE);
  - B. Sputtering;
  - C. Pulsed laser deposition (PLD)
4. Some “chemical” deposition methods:
  - A. Chemical vapor deposition (CVD);
  - B. Techniques involving solutions (CSD, LPE)

**We will restrict to inorganics (organic layers to be mentioned in the future)**

# 1. Overview of some film growth problems I

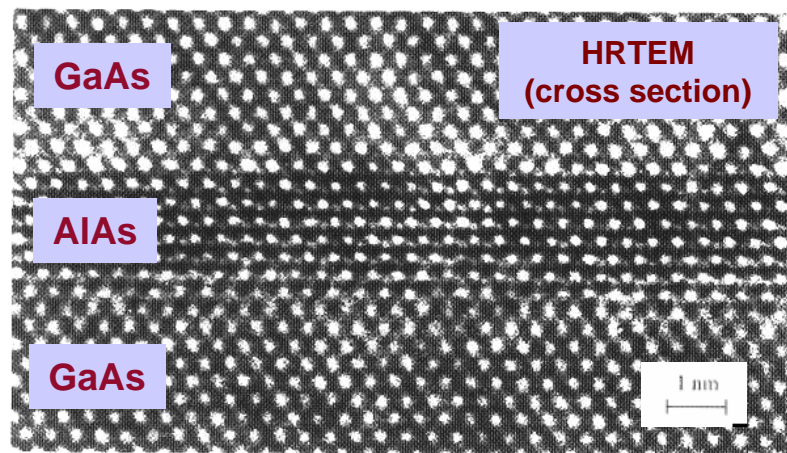
**Thin film:** material layer with thickness  $\ll$  lateral size (typ., 1-100 nm)

Note: besides electronics, thin films are useful for a huge variety of applications (e.g., optics, wear protection, diffusion barriers, mechanics, ...)

In principle, we often aim at growing a thin layer of a (poly)crystalline material either **over a substrate or another layer**

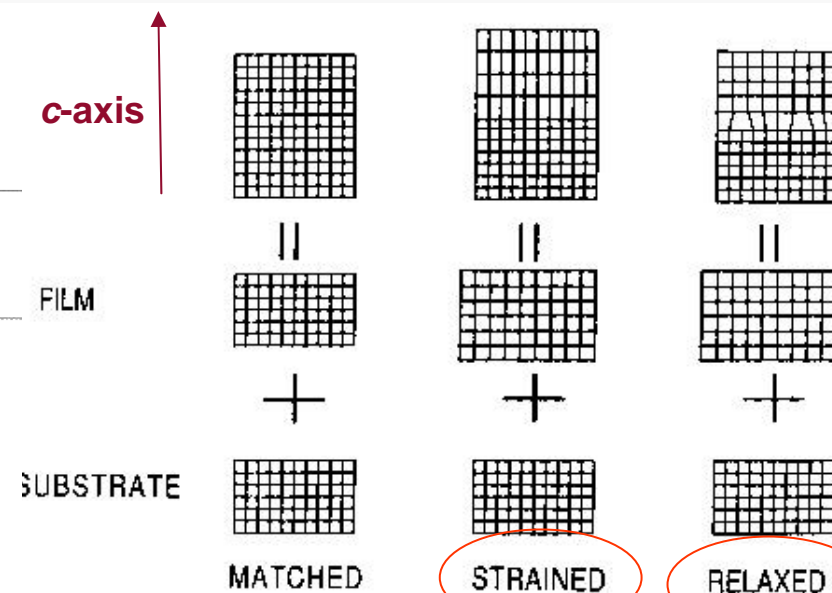
**Homo-epitaxy:** no change in the lattice parameters (i.e., in the material!)

**Hetero-epitaxy** (or pseudo-epitaxy): “slight” changes of the lattice parameters (typ. < 5-10%)



Lattice constants: 5.652 Å (GaAs) 5.3 Å (AIAs)

**Lattice matching is a crucial issue**



Schematic illustration of lattice-matched, strained, and relaxed heteroepitaxy. Homoepitaxy is structurally very similar to lattice-matched heteroepitaxy.

## Overview of some film growth problems II

### “Systematics” of thin film defects

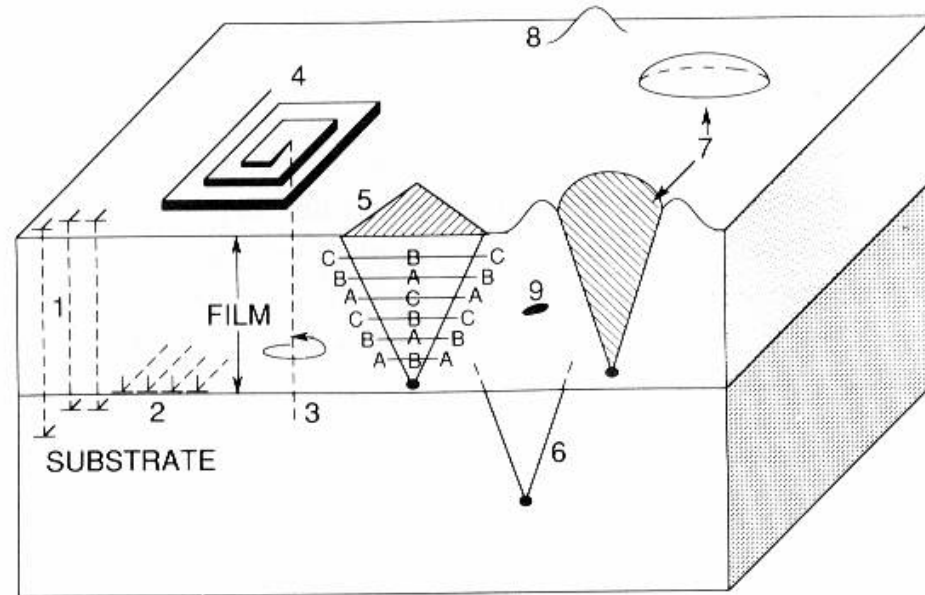


**Figure 7-10.** Schematic composition of crystal defects in epitaxial films: (1) threading edge dislocations; (2) interfacial misfit dislocations; (3) threading screw dislocation; (4) growth spiral; (5) stacking fault in film; (6) stacking fault in substrate; (7) oval defect; (8) hillock; (9) precipitate or void.

**Large variety of defects can occur, often enhanced when nm-sized thickness is concerned**

# A few energetics of heteroepitaxy

If we want to grow an epitaxial film on a different substrate (so-called **heteroepitaxy**), two material parameters have to be considered in addition: the surface energy,  $\gamma$ , and the lattice parameter or lattice match of the two materials. For the case of good lattice match the difference in surface energy leads to two different growth modes as indicated in Figure 8a and b. As long as :

$$\gamma_{\text{layer}} + \gamma_{\text{substrate/layer}} \leq \gamma_{\text{substrate}} \quad (4)$$

we observe perfect wetting and pure layer by layer (or **Frank-van-der-Merve growth**). For the opposite case, we observe island or **Volmer-Weber growth**. For this consideration the surface energies of the crystallographic orientations of actual interest must be applied, which are often not available in data reference tables. If there is a lattice mismatch between substrate and film, an additional growth mode may be observed as indicated in Figure 8c, **Stranski-Krastanov growth**. A first layer may grow matched to the substrate, which yields additional strain energy. With growing thickness this strain energy increases in proportion to the strained volume and an island formation may become more favourable in spite of the larger surface area.

The contributions of strain and surface energy can quite generally be described in a simple model and the resulting difference in energy between island growth and layer growth is given by Eq. (5) and illustrated in Figure 9.

$$\Delta W = W_{\text{surf}} + W_{\text{relax}} = \text{const}_1 \gamma d^2 - \text{const}_2 k \xi^2 d^3 \quad (5)$$

$k$  = bulk modulus,  $\xi$  = strain

Considering films of the same volume content, the increased surface energy for the island growth Figure 8b, is proportional to the island area,  $d^2$ , whereas the energy released by relaxation of the lattice is proportional to the island volume,  $d^3$ . A relaxation mode which is characteristic of isolated islands is shown in Figure 10 for a case where the film material has a larger bulk lattice parameter than the substrate. The model predicts a critical value,  $d_{\text{crit}}$ , where the island growth is finally more favourable and a fast decrease of the energy for larger sizes. However, the limits of the model are reached in this region as the simple relaxation mode is obviously no longer valid for large sizes.

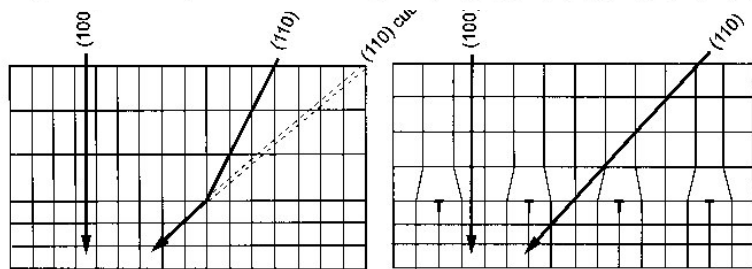
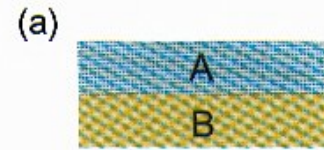
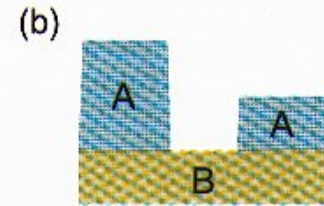


Figure 11: Strain relaxation by misfit dislocations for the example of two initially cubic crystals. As the film has a larger lattice constant than the substrate the forced matching at the interface yields a

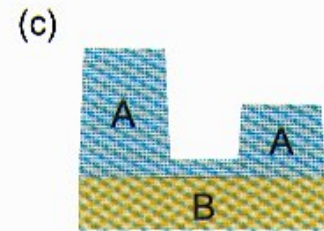
tetragonal distortion of the film. By misfit dislocations this strain can be relaxed and the film can re-approach its cubic structure.



Frank-van-der-Merve



Volmer-Weber



Stranski-Krastanov Favoured by lattice mismatches

Figure 8: Growth modes of the hetero-epitaxy.

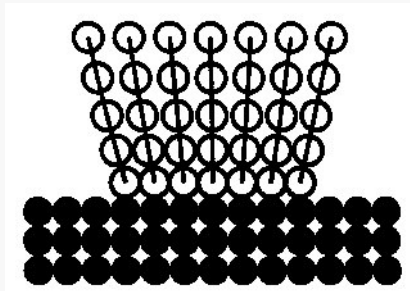


Figure 10: Strain relaxation in pseudo-morphic (dislocation - free) islands.

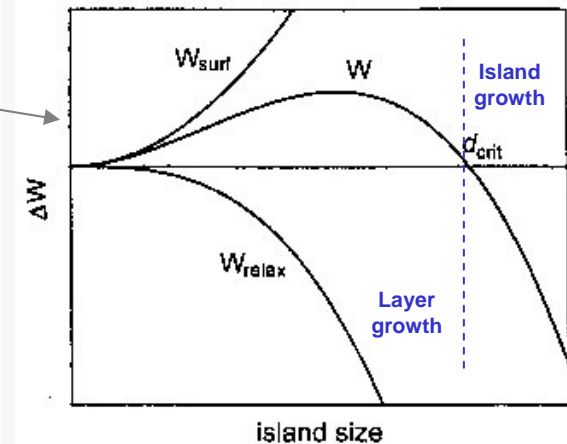


Figure 9: Energy contributions as a function of the island size [5].

**Heteroepitaxy is strongly depending on the "surface energies"**

# A few thermodynamics of adsorption

## 2.3 Film Growth Modes

Nucleation and growth of a film proceeds from energetically favourable places on a substrate surface and even the cleanest polished surface shows some structure. Figure 5 shows schematically the structure of a well-polished single-crystal surface. The characteristic features are the terraces of length,  $l_s$ , the steps and the kinks within the step line, which otherwise runs along well-defined crystallographic directions. If the surface diffusion is fast enough a randomly deposited adatom will diffuse to the energetically most favourable places like steps and especially kinks. If at lower temperatures the diffusion is slower, several mobile adatoms may encounter each other within a terrace and may form additional immobile adatom clusters within the terraces. Similarly, advacancies and their clusters might be formed at the end of the coverage of a terrace. By reducing the step distance and hence the diffusion length by vicinal surfaces, Figure 6, the step controlled growth may be extended to lower temperatures,.

The details of the growth modes for the simplest case of **homoepitaxy**, the growth of a film on a single-crystalline surface of the same material, is indicated in Figure 7. As discussed above, step propagation dominates at higher temperatures and/or small deposition rates and two-dimensional island growth will predominate if immobile clusters are formed by the encounters of mobile adatoms. This simple picture is, however, quite frequently modified: if the jump across the step is kinetically hindered multilayer growth will be observed. This enlarged activation energy for the jump across the step is called the **Ehrlich-Schwoebel effect** and can be understood in a simple model as the adatom is nearly dissociated from the surface in the saddle point of this jump.

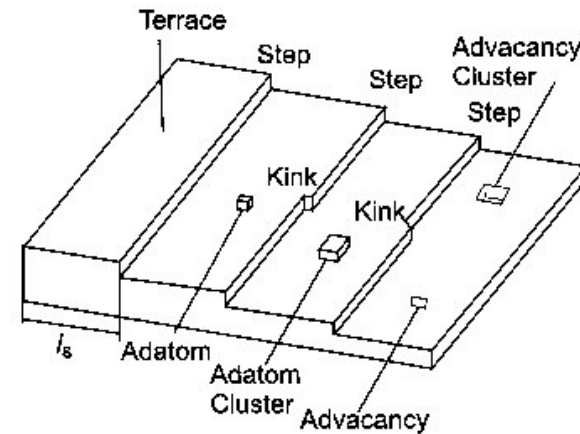


Figure 5: Schematic view of the elements of the surface morphology [3].

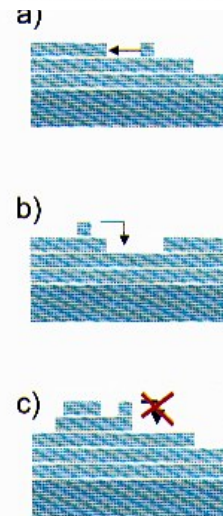


Figure 7: Growth modes of homoepitaxy: (a) step-propagation, (b) 2d-island growth, and (c) multi-layer growth.

We assume arrival of adatoms from vapour (maybe, liquid) phase

Adatom adsorption requires atom energy to be released (e.g., to a kink, or surface defect)

Vicinal surface (engineering of the surface through substrate cutting) can enhance adsorption

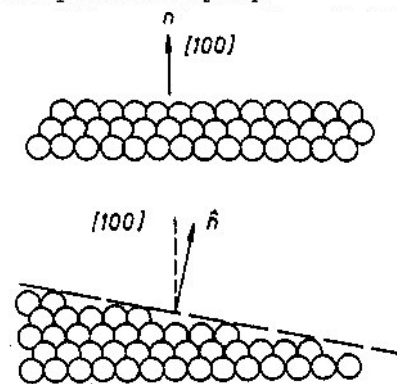
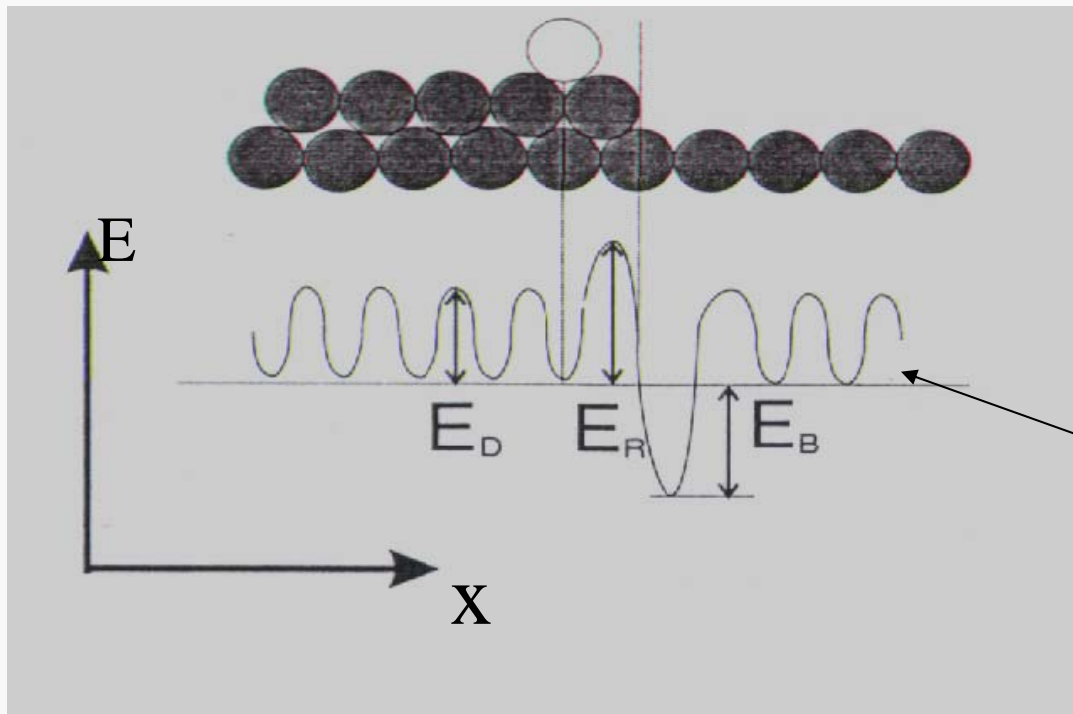


Figure 6: Change of the step distance,  $l_s$ , by cutting a surface at a small angle to a major crystallographic direction, i.e., forming a vicinal surface.

## Diffusion and potential barriers

Thin film formation implies *diffusion* of the impinging particle over the substrate (or the underlying layer)

Material diffusion at the atomistic level is a thermally-activated process involving a *diffusion coefficient*



Diffusion coefficient:

$$D = D_0 \exp(-E/kT)$$

**Modulation at the atom scale of the interaction potential can lead to a barrier (Erwin-Schwoebel) preventing inter-step jumps**

## 2. Nucleation and coalescence

*During a film growth process, when the experimental conditions past the nucleation regime and favor merging of clusters, the system continues to evolve towards a coalescence morphology.*

*In this regime has been characterized the following three cluster growths (Beysens et al.):*

- *Nucleation and individual cluster growth without cluster density reduction or **pre-coalescence** and **transient coalescence** stage (diffusive mass transport limited growth)*
- *Cluster merging or **late stage of coalescence** (static and dynamic)*
- *Secondary nucleation and cluster growth on exposed fraction of surface.*

*This phase of growth is based on spontaneous formation of aggregate of atoms which is large enough to be energetically stable.*

*This condition is reached when the gain in volume energy for an additional monomer exceeds the energy loss due to surface formation*

### ***Kinetic concept (Venable's model)***

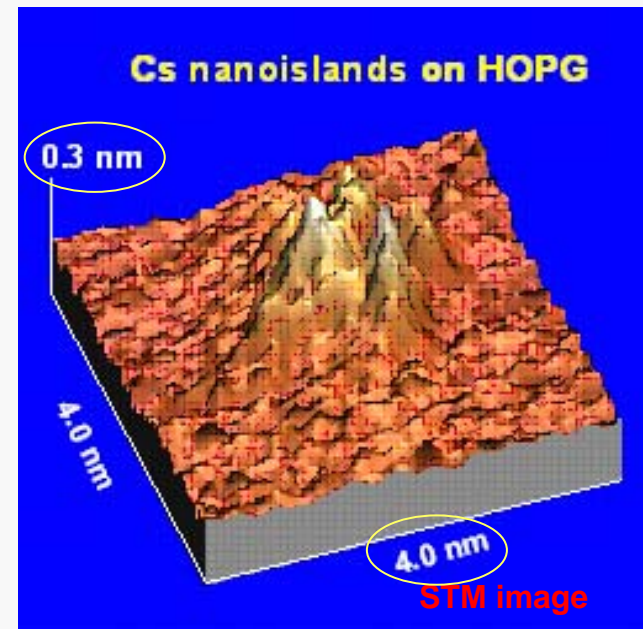
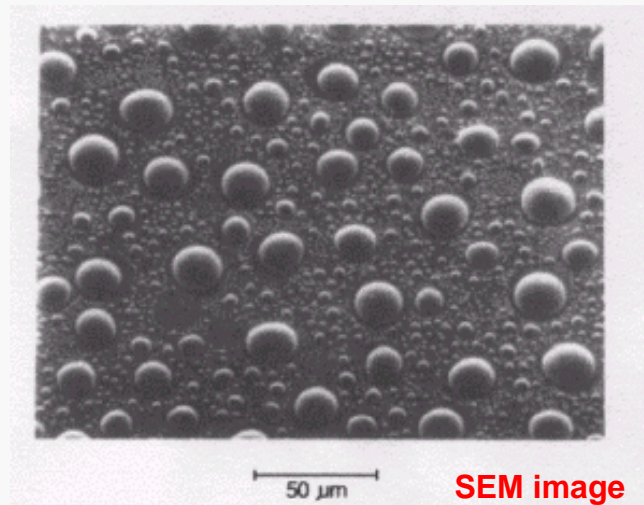
*Critical cluster of size  $i^*$ : adding a further monomer to a critical cluster leads to a stable cluster which does not decompose anymore.*

# Experimental investigation of early growth stages

## *Experimental study of coalescence regime in the system Ga on GaAs(001)*

*(M.Zinke-Allmang et al.)*

- *Base pressure  $< 5 \cdot 10^{-9}$  Pa*
- *Deposition equivalent to a coverage of about 13 monolayers at room temperature.*
- *Annealing temperature = 660°C for 5 min.*

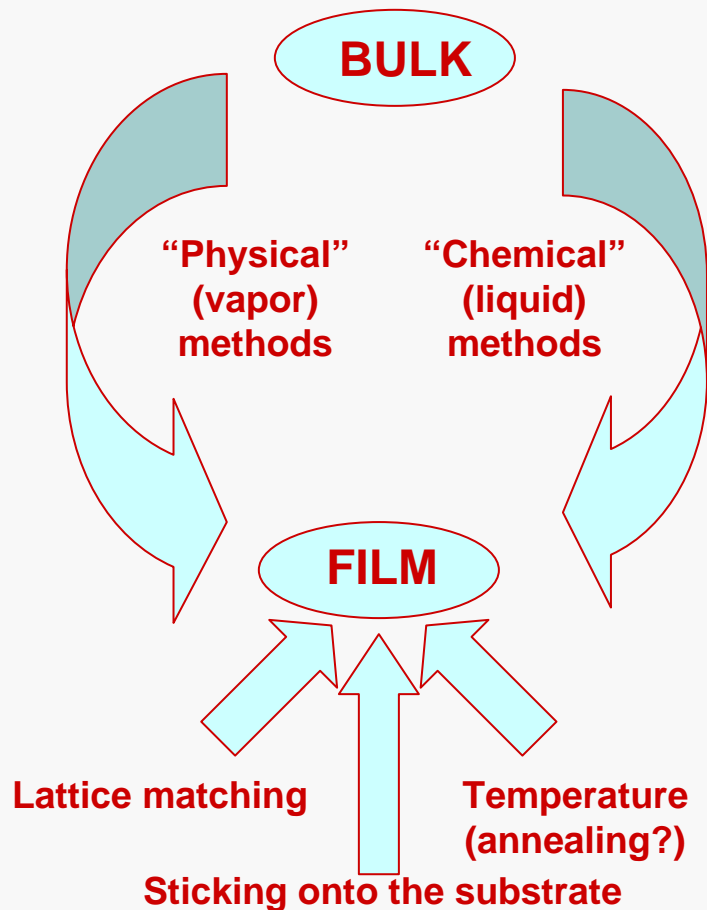


Gallium “prefers” to self-organize in droplets instead of layers (because of energetic reasons)

At moderate coverage rates (~0.1 monolayer) Cesium self-organizes in nanoislands (atoms are from a laser-cooled beam)

# Thin film deposition methods

In general: solid state material is converted into an elemental phase (e.g., atomic, molecular, ...) and let re-aggregate over a substrate (or another layer)



	Physical Vapor Deposition			Chemical Vapor Deposition
	Evaporation / MBE	Sputtering	PLD	CVD / MOCVD
Mechanism of production of depositing species	Thermal energy	Momentum transfer	Thermal energy	Chemical reaction
Deposition rate	High, up to 750,000 Å/min	Low, except for pure metals	Moderate	Moderate Up to 2,500 Å/min
Deposition species	Atoms and ions	Atoms and ions	Atoms, ions and clusters	precursor molecules dissociate into atoms
Energy of deposited species	Low 0.1 to 0.5 eV	Can be high 1-100 eV	Low to high	Low; Can be high with plasma-aid
Throwing power				
a) Complex shaped object	Poor, line of sight	Nonuniform thickness	Poor	Good
b) Into blind hole	Poor	Poor	Poor	Limited
Scalable to wafer size	up to large	up to large	limited	up to large

# Deposition from a vapor

## 2.1 Gas Kinetics

The residual gas pressure in the system is one of the basic parameters to be controlled during film deposition as the residual gas atoms may collide with the depositing species or may hit the growing surfaces and may thus be incorporated in the film, Figure 1. For the simplest assumption that the gas atoms may be considered as not interacting masses with a Maxwell velocity distribution we obtain the mean free path length,  $\lambda$ , of the atoms or molecules

$$\lambda = \frac{1}{\sqrt{2}n\pi d^2} \quad (1)$$

$d$  = molecular diameter,  $N$  = concentration of the gas. With the law of the ideal gas:  $N = p/k_B T$ ,  $k_B$  = Boltzmann constant, we obtain:

$$\lambda = \frac{k_B T}{\sqrt{2}p d^2} \quad (2)$$

For the example of air molecules we obtain a free path length which is of the order of a typical distance from source to substrate of about 20 cm at a pressure of  $0.5 \cdot 10^{-3}$  mbar. This rather moderate vacuum level shows that the beam interaction is not a critical condition for the base vacuum. More critical is the number of residual gas atoms which hit the growing surface and limit the purity of the film if they are incorporated. This number can be expressed as

$$N_i = p_i \sqrt{\frac{1}{2\pi k_B m_i T}} \quad (3)$$

$m_i$  = atomic or molecular mass. Typical results are summarized in Tab. 2. Assuming a sticking coefficient of unity, the incorporation of residual gas atoms may be expressed in terms of monolayers and this growth rate may be rather high as compared to a typical growth rate of an epitaxial film i.e., one monolayer / s. Hence, for clean films ultra-high vacuum (UHV, better than  $10^{-9}$  mbar) may be necessary.

$p$ , mbar	Mean free path, cm (between collisions)	Collisions / s (between molecules)	Molecules/(cm <sup>2</sup> s) (sticking surface)	Monolayer / s*
$10^0$	$6.8 \cdot 10^{-3}$	$6.7 \cdot 10^6$	$2.8 \cdot 10^{20}$	$3.3 \cdot 10^5$
$10^{-3}$	$6.8 \cdot 10^0$	$6.7 \cdot 10^3$	$2.8 \cdot 10^{17}$	$3.3 \cdot 10^2$
$10^{-6}$	$6.8 \cdot 10^3$	$6.7 \cdot 10^0$	$2.8 \cdot 10^{14}$	$3.3 \cdot 10^{-1}$
$10^{-9}$	$6.8 \cdot 10^6$	$6.7 \cdot 10^{-3}$	$2.8 \cdot 10^{11}$	$3.3 \cdot 10^{-4}$

\* Assuming the condensation coefficient is unity

Table 2: Some facts about residual air at 25 °C in a typical vacuum used for film deposition (after Chopra [2]).

## 2.2 Thermodynamics

Phase-diagrams are the starting point for considering the deposition of a new material in order to see the stability range of the envisaged phase and the existence of concurrent phases. Standard phase diagrams are given at ambient pressure, however, changes with pressure must be considered for vacuum deposition methods. Figure 3 shows as a simple example the phase diagram of the completely intermixing binary system Si-Ge and the change from ambient pressure down to the UHV region [3]. At 1 mbar there is not much change compared to atmospheric pressure and we observe a wide range of stability of the mixed homogeneous crystalline phase, c, of Si-Ge (the decomposition of this homogeneous phase at very low temperature is somewhat speculative). At higher temperatures the liquid, l, to solid (crystalline) phase transition is indicated and above 2000 K the liquid to vapour, v, transition is shown. With decreasing pressure there is a strong decrease in temperature of the l-v borderlines and even an overlap with the c-l lines. Finally, in the UHV region,  $10^{-9}$  mbar, the liquid has disappeared and only direct sublimation, c, v is left at temperatures around 1100 K. Hence, re-evaporation of the material under UHV conditions and high temperatures must be considered. In addition, a comparison with the deposition rates and gas pressures discussed along with Table 2 shows that the deposition of the films usually proceeds under high supersaturation, i. e. condi-

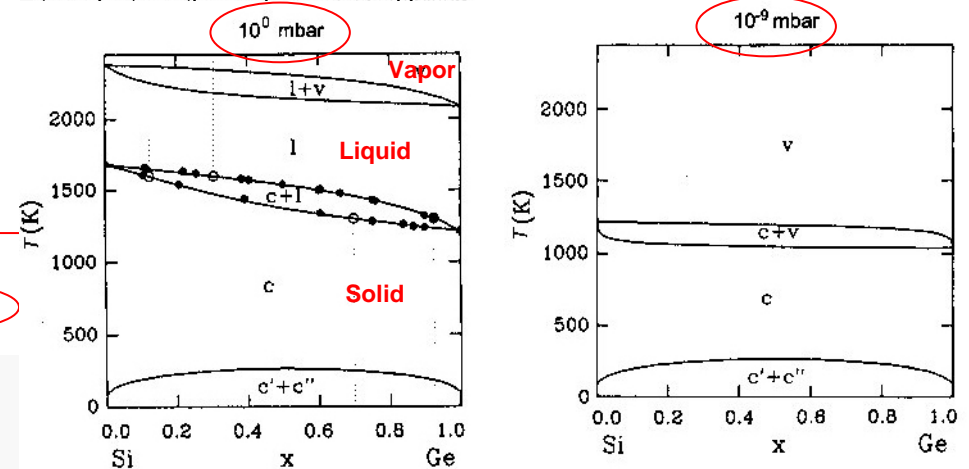
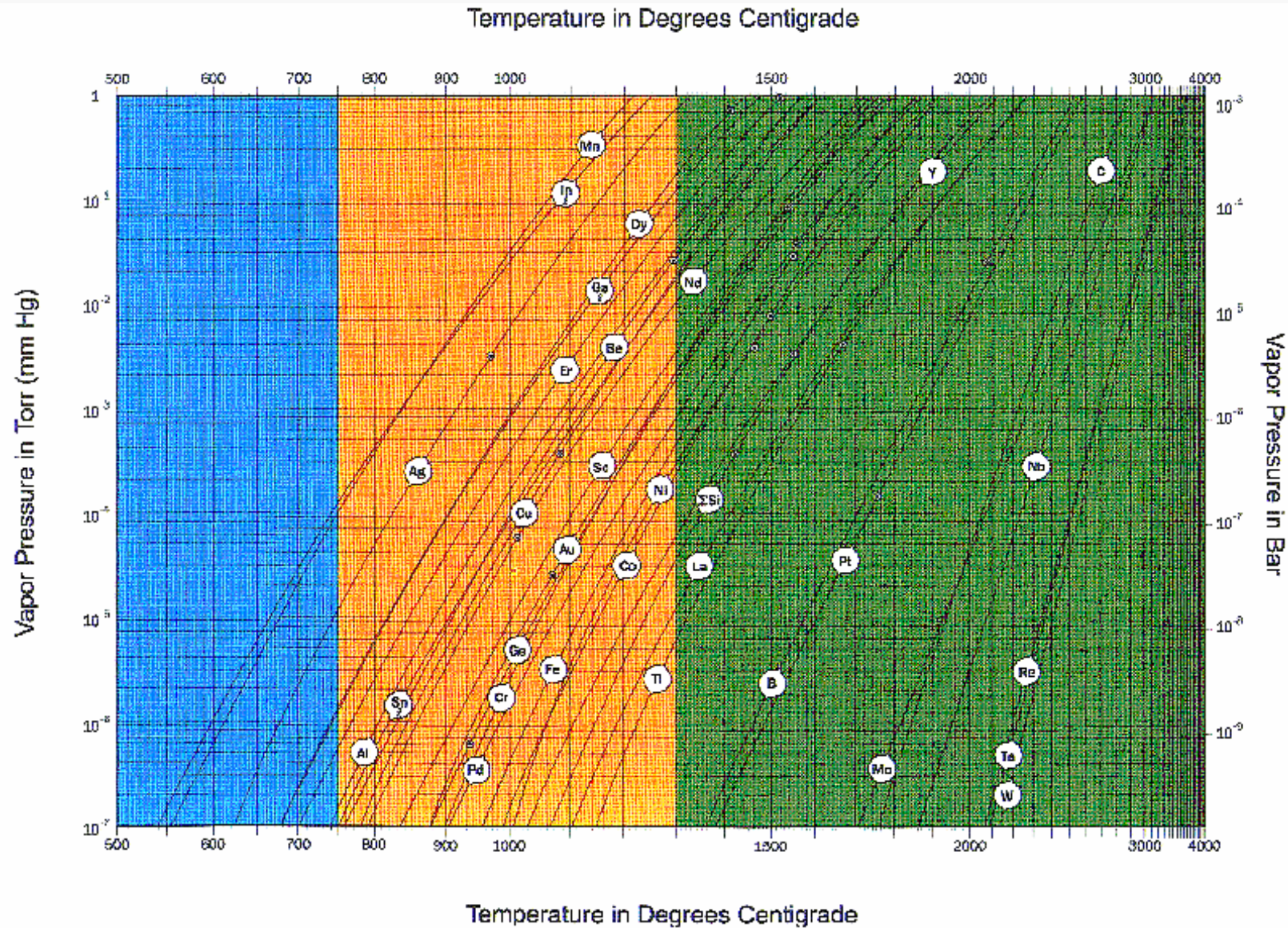


Figure 3: x-T phase diagram of the  $Si_{(1-x)}-Ge_x$  systems at  $10^0$  and  $10^{-9}$  mbar [3].

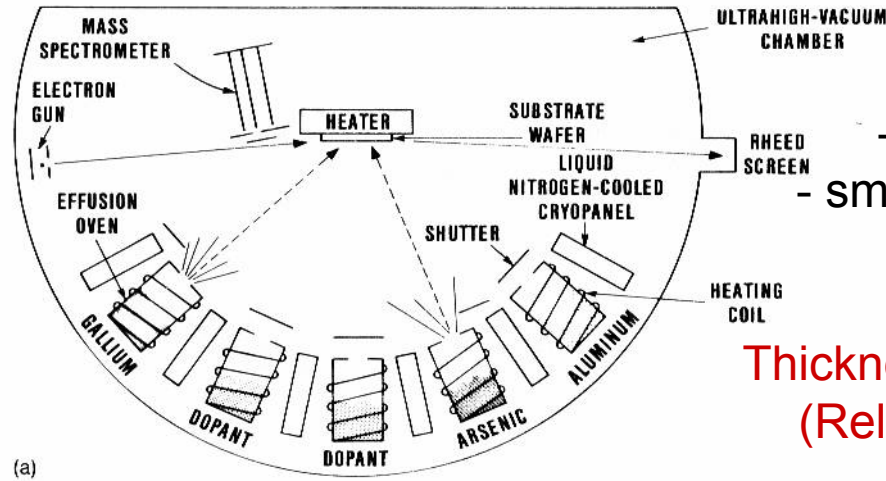
**UHV conditions improve purity and affect phase diagrams**

# Effusive vaporization

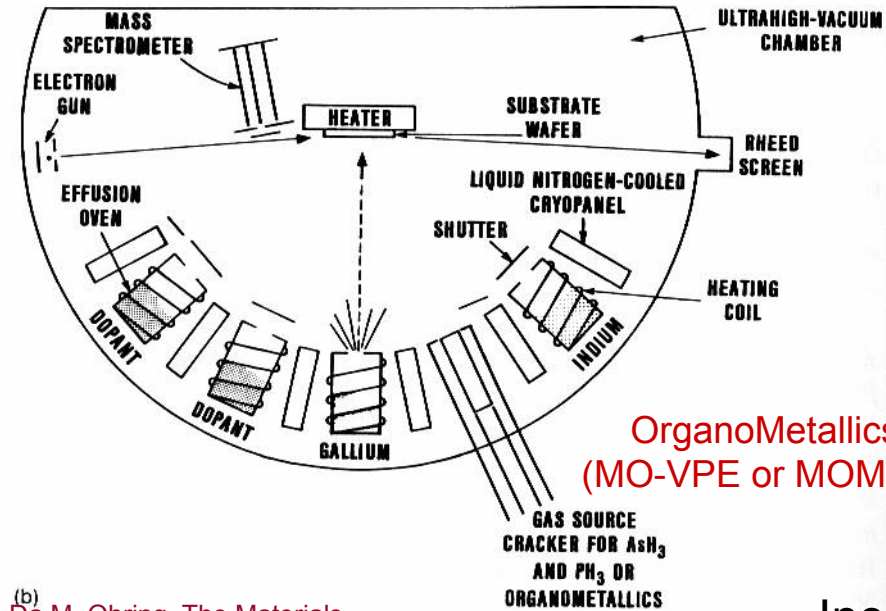


**(Effusive) atomic beams can be produced by simply (?) heating a solid bulk**

### 3.A. Molecular Beam Epitaxy: MBE, MOMBE



(a)

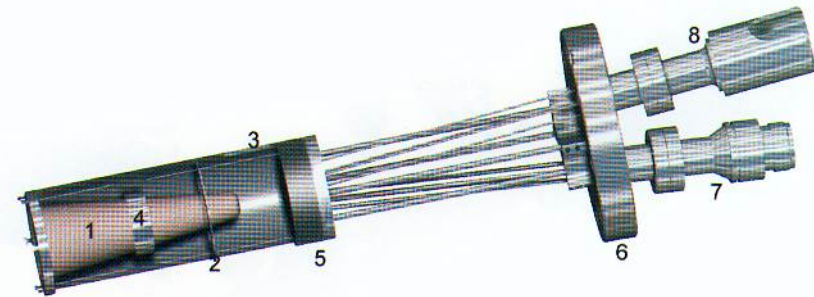


(b)

Da M. Ohring, The Materials Science of Thin Films, Academic (1992)

- Key points for MBE:
- clean process (UHV,  $p \leq 10^{-10}$  mbar)
  - small continuous deposition rate ( $\sim 1 \mu\text{m/h}$ )
  - suitable with semiconductor

Thickness easily controlled at the monolayer level  
 (Relatively) low kinetic energy favors epitaxy  
 Heterostructures easily fabricated



Example of effusive oven (MPI)

Inert materials used (but difficult with oxides!)

# MBE sources

## 3.1.1 Sources

The schematic of the classical MBE source, the Knudsen cell, is illustrated in Figure 13. The evaporation rate,  $N_e$ , is described by the Hertz-Knudsen (or Langmuir) equation:

$$N_e = \frac{p_e A_e}{\sqrt{2\pi m k_B T}} \quad (6)$$

$p_e$  is the equilibrium vapour pressure and  $A_e$  the area of the aperture [7]. Therefore, the source can be precisely controlled by a single parameter, the temperature. However, the technical details are very complex and involve more parameters than shown in Eq. (6).

Figure 14 shows the principle of an electron beam evaporator. The electron beam is magnetically deflected by 270° and is centred on the source material. In this way a melt of the source material is produced on a block of the same material which can be held in a water-cooled cold crucible in order to avoid contamination of the melt.

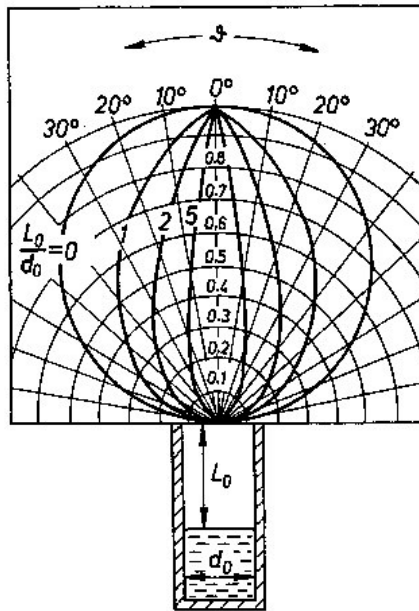


Figure 13: Schematics of a Knudsen cell and the distribution of the vapour beam intensity [7]. The distribution depends on the ratio  $L_0/d_0$  and consequently on the filling level of the cell.

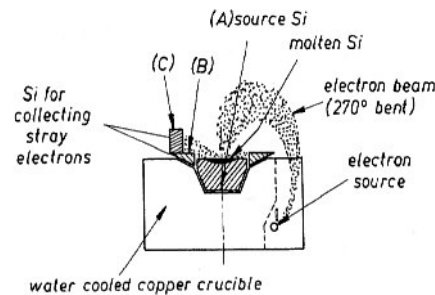


Figure 14: Schematics of an electron beam evaporator for Si evaporation [7]; B: Si guard ring, C: catcher for backscattered electrons.

Da M. Ohring, *The Materials Science of Thin Films*, Academic (1992)

Consider now a substrate positioned a distance  $l$  from a source aperture of area  $A$ , with  $\phi = 0$ . An expression for the number of evaporant species striking the substrate is

$$\dot{R} = \frac{3.51 \times 10^{22} PA}{\pi l^2 (MT)^{1/2}} \text{ molecules/cm}^2\text{-sec.} \quad (7-13)$$

As an example, consider a Ga source in a system where  $A = 5 \text{ cm}^2$  and  $l = 12 \text{ cm}$ . At  $T = 900 \text{ }^\circ\text{C}$  the vapor pressure  $P_{\text{Ga}} \approx 1 \times 10^{-4} \text{ torr}$ , and substituting  $M_{\text{Ga}} = 70$ , the arrival rate of Ga at the substrate is calculated to be  $1.35 \times 10^{14} \text{ atoms/cm}^2\text{-sec}$ . The As arrival rate is usually much higher, and, therefore, film deposition is controlled by the Ga flux. An average monolayer of GaAs is  $2.83 \text{ \AA}$  thick and contains  $\sim 6.3 \times 10^{14} \text{ Ga atoms/cm}^2$ . Hence, the growth rate is calculated to be  $(1.35 \times 10^{14}) / (6.3 \times 10^{14}) \times 2.83 \times 60 = 36 \text{ \AA/min}$ , a rather low rate when compared with VPE.

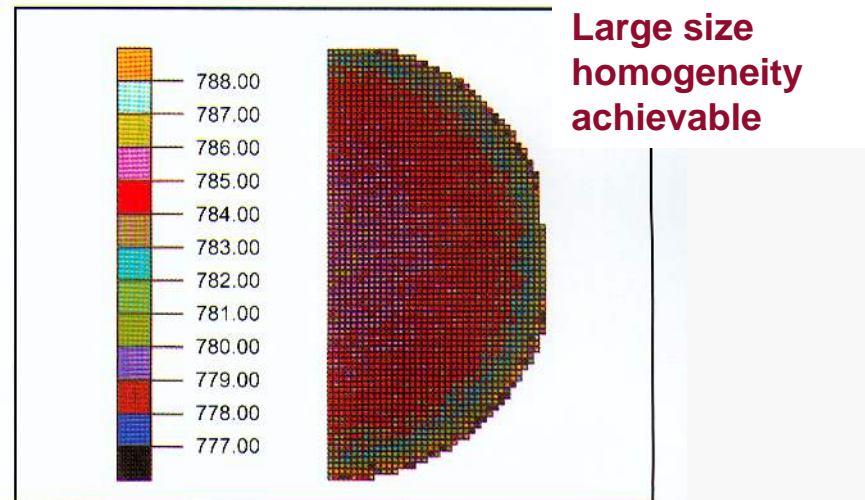
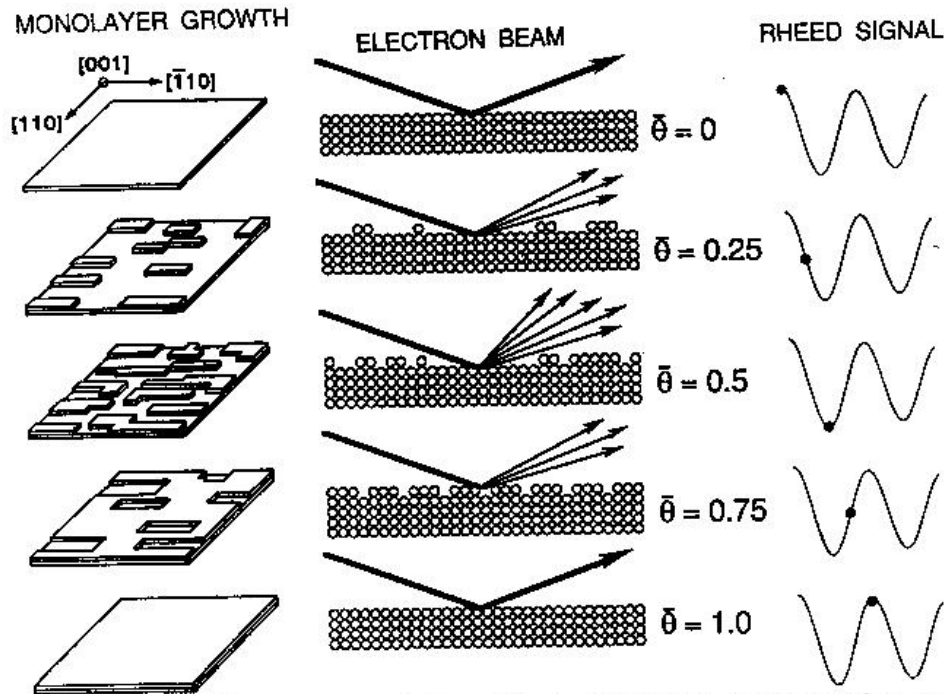


Figure 4-3: Thickness uniformity across a 3" wafer represented as a mapping of quantum well photoluminescence. The MQW structure was grown using a SUMO Ga cell in a MOD GEN II system. Uniformity better than  $\pm 1\%$  was achieved. Data courtesy R. Sacks, Ohio State University and K. Stair, Northwestern University.

## In-situ thickness control

Rutherford High Energy Electron Diffraction (RHEED) frequently used to diagnose film coverage and to measure film thickness



**Figure 7-22.** Real space representation of the formation of a single complete monolayer;  $\bar{\theta}$  is the fractional layer coverage; corresponding RHEED oscillation signal is shown.

### Coherent/incoherent Bragg interference

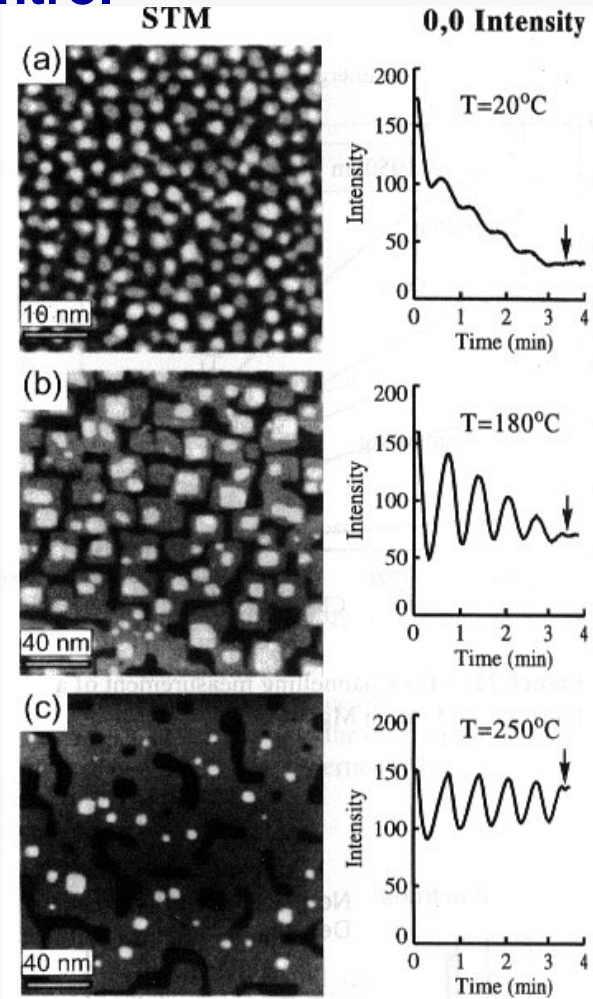
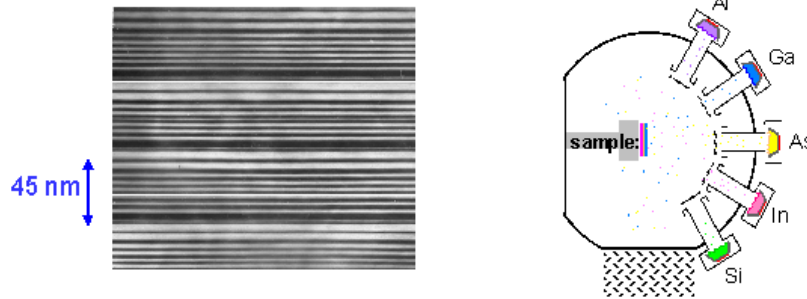


**Figure 19:** STM and RHEED results for the homo-epitaxial growth of Fe films on Fe(100) substrates. The growth was interrupted after 5 oscillations, as indicated by the arrow. The scale of the STM was changed between part a and b! The roughness of the films decreases strongly with temperature: rms (root mean square) amplitude 0.116 nm, 0.095 nm and finally at 250°C 0.06 nm [9].

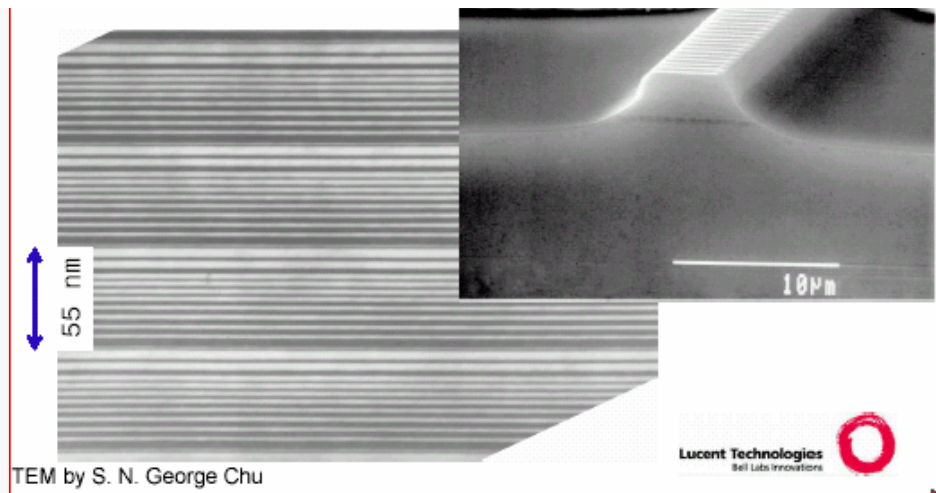
# Successes and main limitations of MBE

QC-laser crystal grown by  
Molecular Beam Epitaxy (MBE)



Cross-section of a few stages of QC-laser crystal crystal growth one atomic layer at a time

- ◆ Many (~ 500), few-atoms thick layers of alloy materials (Al, Ga, As, In);
- ◆ atomic control of layer thickness, 1 nanometer (nm) = 4 atomic layers
- ◆ atomically flat layer interfaces



TEM by S. N. George Chu

MBE is able to produce homogeneous layers with a very well controlled thickness and extremely low roughness (see, for instance, the success of quantum cascade lasers)

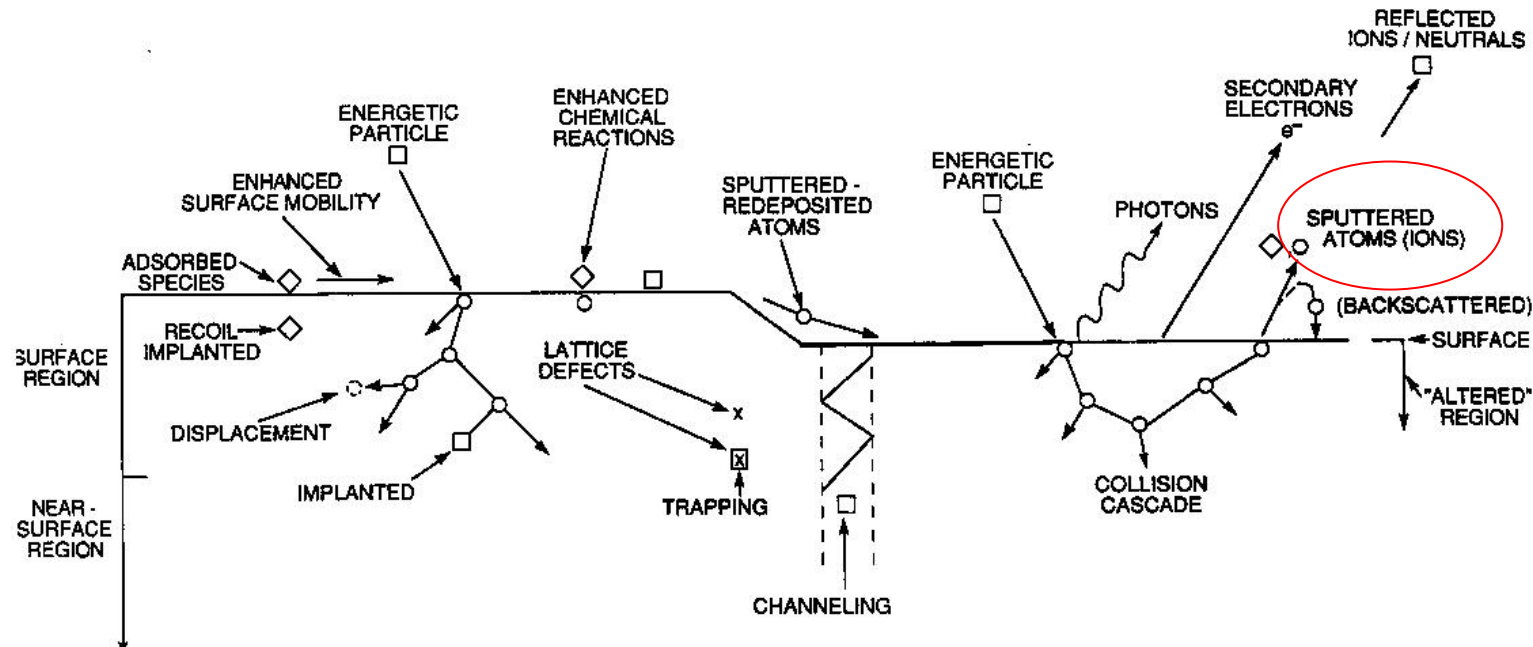
...**BUT**...

Main limitations of MBE (from the nanotechnological point of view):

- poor suitability with refractory materials (too high temperature);
- poor suitability with complex materials (e.g., reactivity with oxygen);
- low kinetic energy of the particles and need for an annealing treatment

## 3.B. Sputtering and charge bombardment

Charged particles (ions or electrons) electrically accelerated towards the surface of a bulk target lead to material desorption and vaporization (not only elemental, though)



Da M. Ohring, *The Materials Science of Thin Films*, **Figure 3-16**. Depiction of energetic particle bombardment effects on surfaces and growing films. (From Ref. 18). Academic (1992)

Main advantages:

- efficient also with “refractory” materials (e.g., ceramics, some metals with large vaporization temperature)
- large growth rate (up to several  $\mu\text{m}/\text{h}$ )

# DC, RF, Magnetron sputtering

Charges typically belong to (or form) a plasma of an inert gas (e.g., Ar) produced by CW or RF excitation

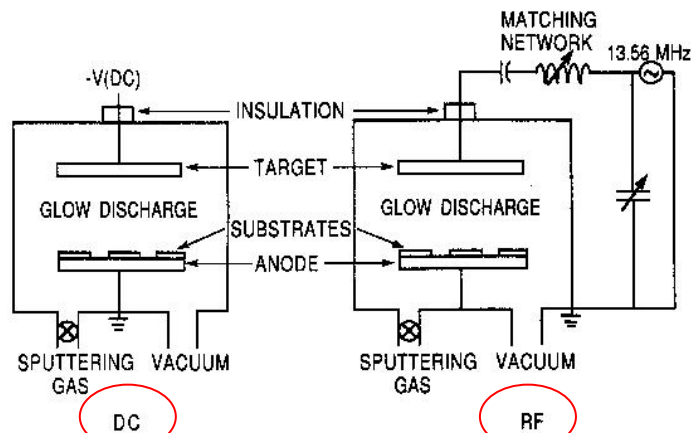


Figure 3-13. Schematics of simplified sputtering systems: (a) dc, (b) RF.

Table 3-4. Sputtering Yield Data for Metals (atoms/ion)

Sputtering Gas Energy (keV)	He	Ne	Ar	Kr	Xe	Ar	Ar Threshold Voltage (eV)
Ag	0.20	1.77	3.12	3.27	3.32	3.8	15
Al	0.16	0.73	1.05	0.96	0.82	1.0	13
Au	0.07	1.08	2.40	3.06	3.01	3.6	20
Be	0.24	0.42	0.51	0.48	0.35		15
C	0.07	—	0.12	0.13	0.17		
Co	0.13	0.90	1.22	1.08	1.08		25
Cu	0.24	1.80	2.35	2.35	2.05	2.85	17
Fe	0.15	0.88	1.10	1.07	1.00	1.3	20
Ge	0.08	0.68	1.1	1.12	1.04		25
Mo	0.03	0.48	0.80	0.87	0.87	1.13	24
Ni	0.16	1.10	1.45	1.30	1.22	2.2	21
Pt	0.03	0.63	1.40	1.82	1.93		25
Si	0.13	0.48	0.50	0.50	0.42	0.6	
Ta	0.01	0.28	0.57	0.87	0.88		26
Ti	0.07	0.43	0.51	0.48	0.43		20
W	0.01	0.28	0.57	0.91	1.01		33

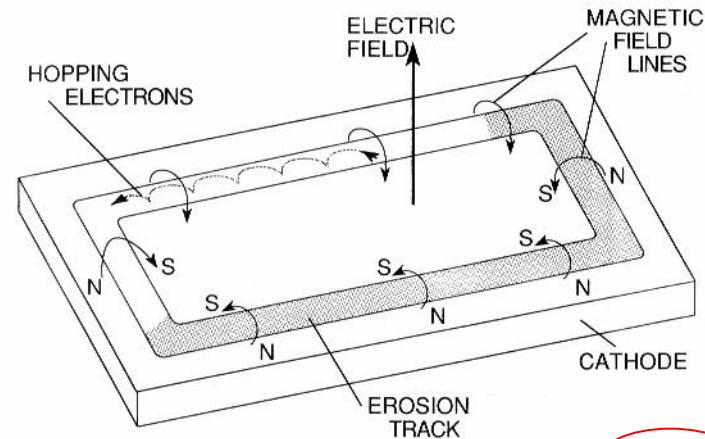


Figure 3-21. Applied fields and electron motion in the planar magnetron.

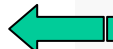
In **magnetron**, magnetic fields do enhance collisional processes in the plasma, so improving the overall process efficiency

## Main disadvantages:

- Presence of a foreign gas → purity issues
- Backscattering possibility → film damage
- Scarce efficiency of atomization → poor control of the growth (i.e., thickness and compositional homogeneity)

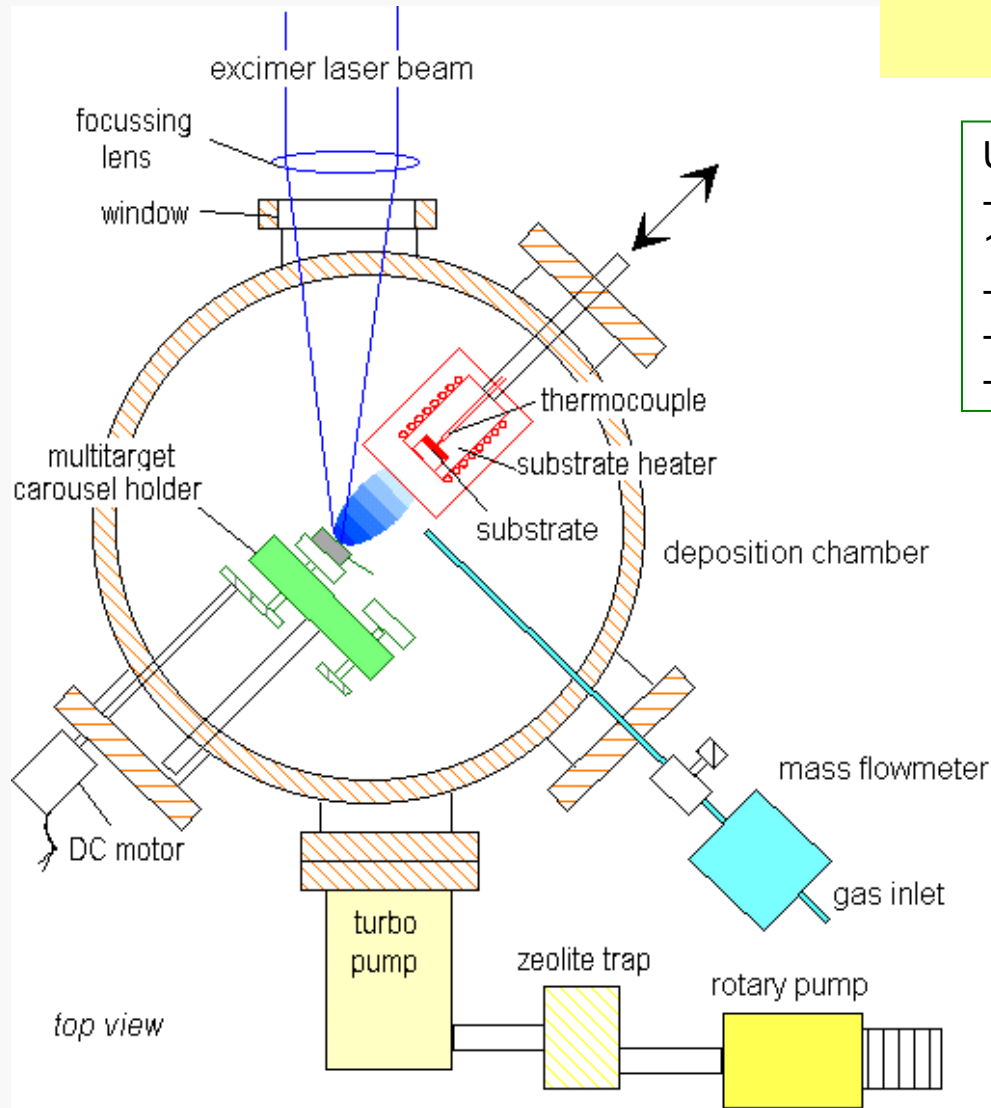
# Sputtering vs vaporization

Da M. Ohring, The Materials Science of Thin Films, Academic (1992)

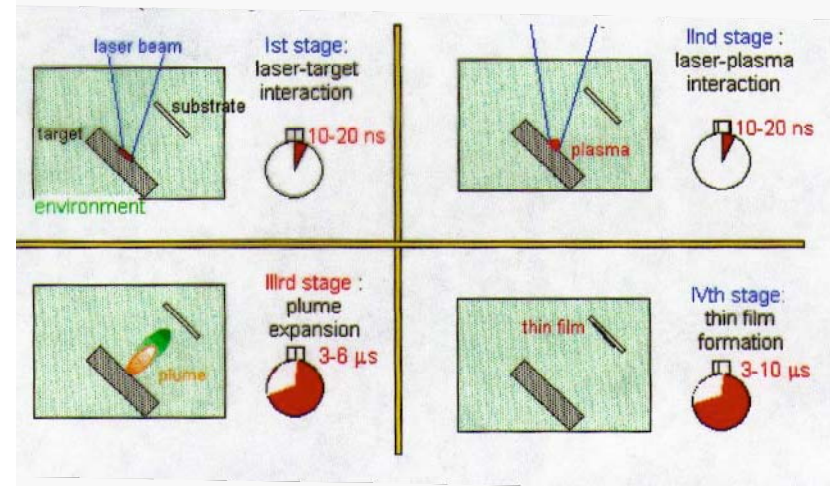
Evaporation	Sputtering
<b>A. Production of Vapor Species</b>	
1. Thermal evaporation mechanism	1. Ion bombardment and collisional momentum transfer
2. Low kinetic energy of evaporant atoms (at 1200 K, $E = 0.1$ eV)	2. High kinetic energy of sputtered atoms ( $E = 2-30$ eV) 
3. Evaporation rate (Eq. 3-2) (for $M = 50$ , $T = 1500$ K, and $P_e = 10^{-3}$ ) $\approx 1.3 \times 10^{17}$ atoms/cm <sup>2</sup> -sec.	3. Sputter rate (at 1 mA/cm <sup>2</sup> and $S = 2$ ) $\approx 3 \times 10^{16}$ atoms/cm <sup>2</sup> -sec
4. Directional evaporation according to cosine law	4. Directional sputtering according to cosine law at high sputter rates 
5. Fractionation of multicomponent alloys, decomposition, and dissociation of compounds	5. Generally good maintenance of target stoichiometry, but some dissociation of compounds. 
6. Availability of high evaporation source purities 	6. Sputter targets of all materials are available; purity varies with material 
<b>B. The Gas Phase</b>	
1. Evaporant atoms travel in high or ultrahigh vacuum ( $\sim 10^{-6}-10^{-10}$ torr) ambient	1. Sputtered atoms encounter high-pressure discharge region ( $\sim 100$ mtorr)
2. Thermal velocity of evaporant $10^5$ cm/sec	2. Neutral atom velocity $\sim 5 \times 10^4$ cm/sec 
3. Mean-free path is larger than evaporant-substrate spacing. Evaporant atoms undergo no collisions in vacuum 	3. Mean-free path is less than target-substrate spacing. Sputtered atoms undergo many collisions in the discharge
<b>C. The Condensed Film</b>	
1. Condensing atoms have relatively low energy	1. Condensing atoms have high energy 
2. Low gas incorporation	2. Some gas incorporation 
3. Grain size generally larger than for sputtered film	3. Good adhesion to substrate
4. Few grain orientations (textured films) 	4. Many grain orientations

### 3.C. Pulsed Laser Deposition (PLD)

**“Collisions” with energetic photons lead to:**  
**- bond breaking;**  
**- local and abrupt material heating**



UV laser sources:  
 - excimer (XeCl 308nm, KrF 248nm, ArF 193nm,...)  
 - Nd-YAG 1064 nm (III or IV harmonics)  
 - pulse duration: ~ 10 ns (sub-ns as well, even fs)  
 - fluence: 1-5 J/cm<sup>2</sup> (i.e., hundreds of MW/cm<sup>2</sup>)



Pulsed process with different steps

# Features of the laser/target coupling

Electron nature of the interaction → *non-thermal vaporization*

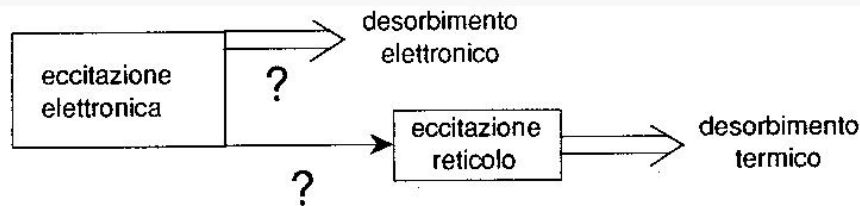


Fig. 2.3. Schema dell'approccio microscopico al problema dell'interazione laser-materia.

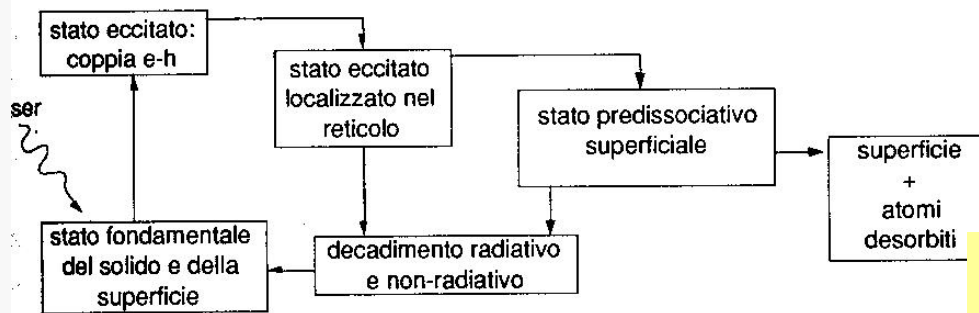


Fig. 2.4. Schema dei processi di interazione laser-materia che conducono alla liberazione di materiale dalla superficie di un target dielettrico (adattata da [37]).

Materiale	YBCO	Si	Ni
Conducibilità termica ( $W\ cm^{-1}\ K^{-1}$ )	0.025	$1600 \times T^{-1.23}$ , $T < 1370\ K$ $0.2$ , $T > 1370\ K$	$11 \times T^{-0.4}$ , $T < 630\ K$ $0.08 \times T^{0.3}$ , $630 < T < 1726\ K$
Coefficiente di assorbimento ( $cm^{-1}$ )	$1.75 \times 10^5$	$> 1.5 \times 10^6$	$1.0 \times 10^6$
Riflettività (per $\lambda_L = 308\ nm$ )	0.11	0.59 0.73 (fase liquida)	0.40 0.70 (fase liquida)
Temperatura di evaporazione (K)	1900	3400	3187
Calore latente ( $J/cm^2$ )	14940	4206	2660
Calore specifico ( $J/cm^3\ K$ )	2.46	$2 \times T^{-3.68}$	$0.72 \times T^{0.3}$ , $T < 630\ K$ $0.5 \times T^{0.3}$ , $T > 630\ K$

Tab. 2.1. Valori dei parametri termofisici ed ottici per diversi materiali (da [52, 53]).

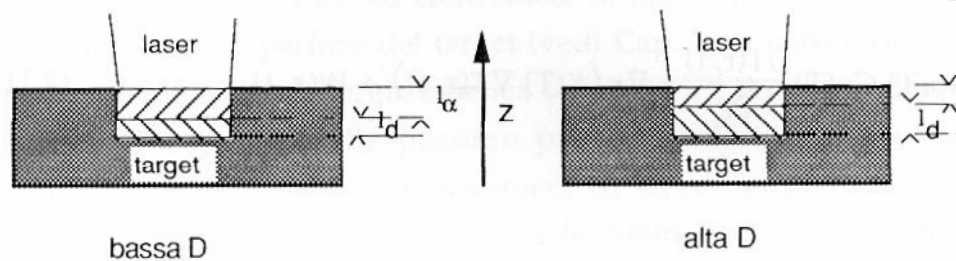


Fig. 2.7. Range di assorbimento di radiazione  $l_\alpha$  e di diffusione del calore in materiali con bassa ed alta diffusività termica  $D$  (a sinistra e destra nella figura rispettivamente); indicato è anche l'asse  $z$  considerato nel testo.

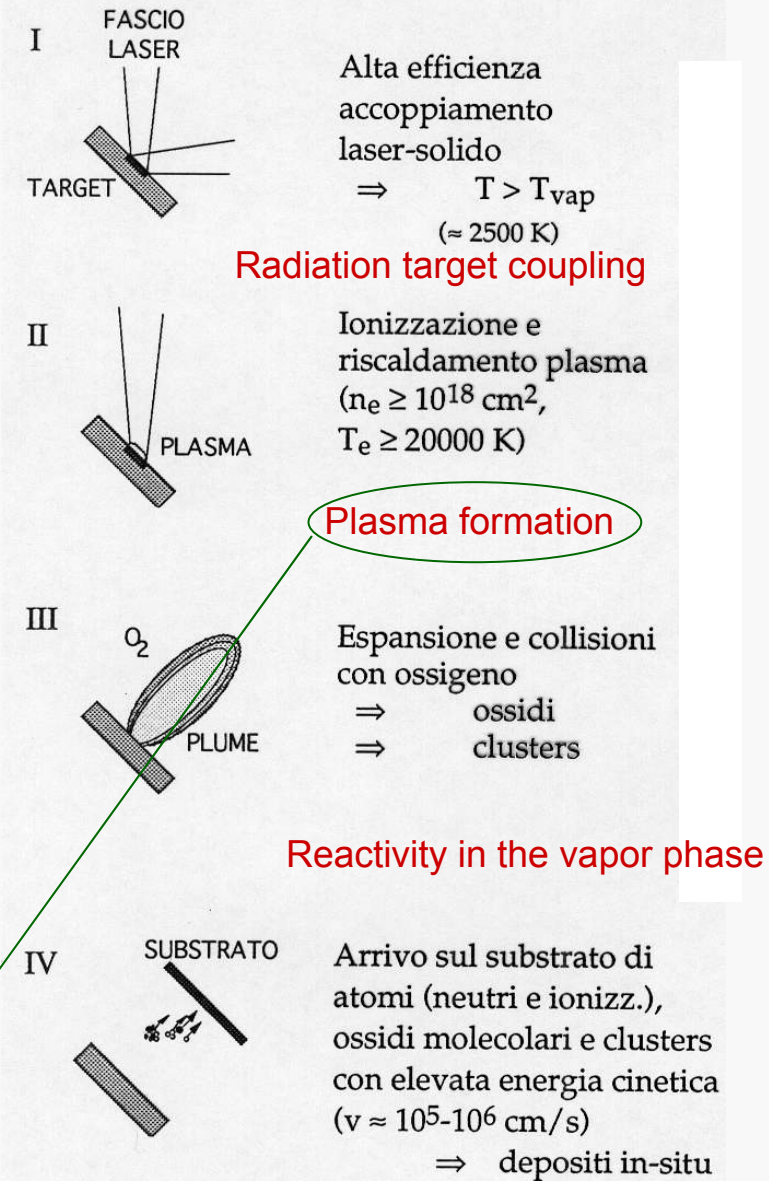
- Some PLD pros:**
- ✓ Huge efficiency with virtually any kind of materials;
  - ✓ Highly localized interaction (reduced target damage);
  - ✓ Congruency of film and target composition
  - ✓ Excellent flexibility (ablation source is outside the deposition chamber and a foreign gas can be either used or not used)

## Some peculiarities of PLD

PLD is a *pulsed* process

1. UV laser energy is efficiently transferred to the target
2. A plasma is formed following interaction of the laser pulse with the vaporized material
3. Vaporized material (plume) expands in a highly peaked beam
4. High energy elemental materials impinges onto the substrate favoring thin film formation even without post-annealing.

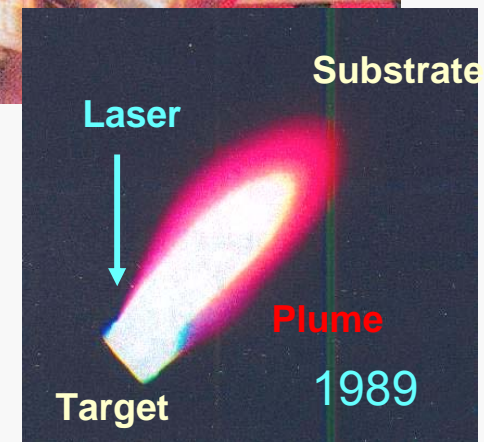
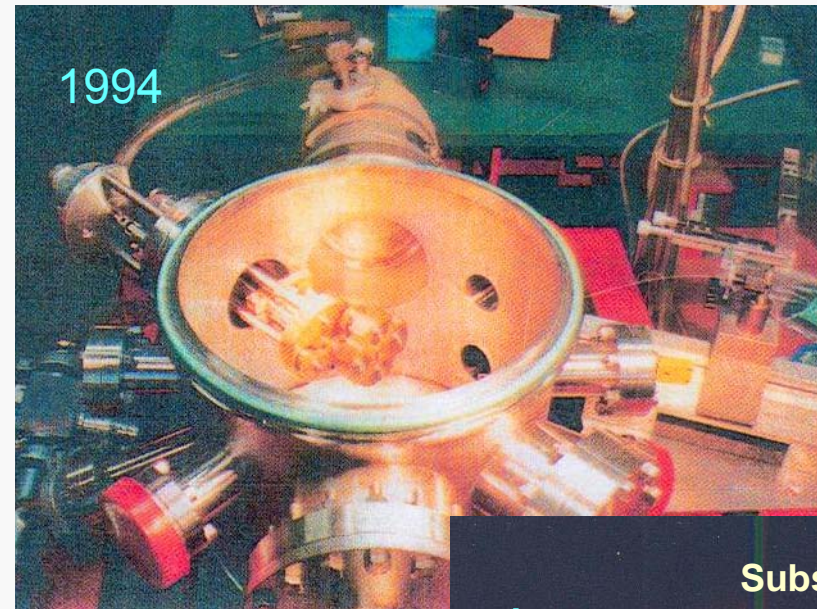
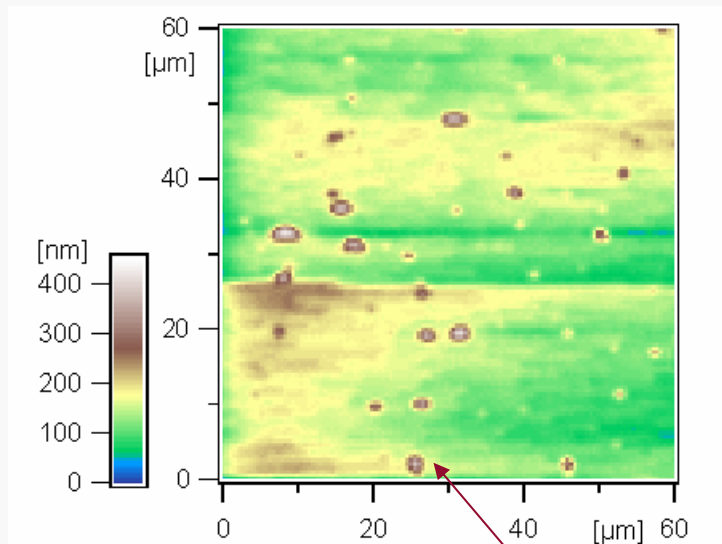
*This step is practically absent when using ultrashort (sub-ps) laser pulses*



**Arrival of high energy particles onto the substrate**

## Main limitations of PLD

PLD broadly and rapidly diffused (starting from late 80's) in worldwide labs for production of films of "difficult" materials (e.g., superconductive and ferroelectric ceramics, nitrides, silicides, carbides and other hard coatings)  
It can be used also for nanoparticles formation (we have seen PLD in fullerenes and CNTs)



Some **disadvantages** of PLD:

- Relatively small areas are covered ( $\sim \text{cm}^2$ )
- Rather poor surface homogeneity (*droplets*)
- Rather poor overall efficiency (i.e., growth rate)

## 4.A. Chemical Vapor Deposition (CVD)

### 4 Chemical Deposition Methods

Chemical deposition generally includes **chemical solution deposition (CSD)** as well as **chemical vapour deposition (CVD)**. In both cases, **chemical precursors are employed** which undergo chemical reactions for the formation of the film. We will place special emphasis on CVD as this method finally allows the deposition of ultrathin films and the **conformal deposition** on complex-shaped structures which are essential for ULSI. CSD includes sol-gel techniques and metal-organic decomposition MOD and typically uses spin-on techniques for the distribution of a solute film which is subsequently processed and crystallized. Finally, we give a short introduction to a very different method for deposition from solutions, the **Langmuir-Blodgett (LB)** technique. LB techniques allow the deposition of monomolecular organic films on different substrates making use of the hydrophilic/hydrophobic orientation of the molecules.

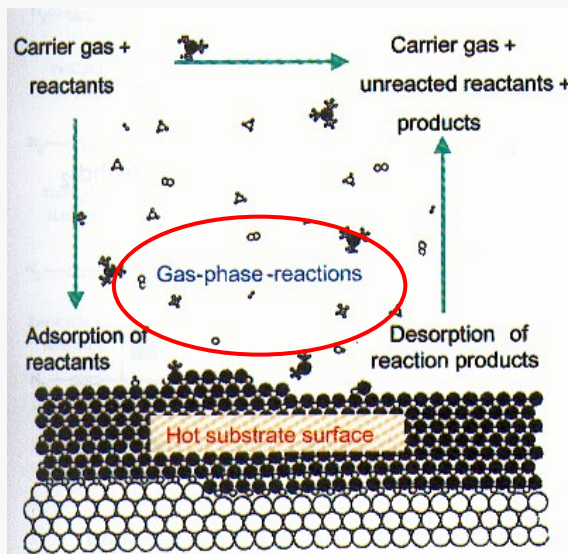


Figure 30: Schematics of the gas flow and the atomic scale chemical environment in the region of the growing film surface during a MOCVD process.

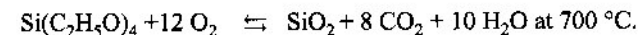
Chemical reactions are realized in the vapour phase, the resulting compounds are deposited onto a substrate acting as an energy reservoir for the reactions and unwanted products are carried away

#### 4.1 Chemical Vapour Deposition

The general principles of CVD are well established and a number of reviews and textbooks are available [20], [21], [22], which cover many generic issues common to any type of material. In CVD, film growth occurs through the chemical reaction of the component chemicals (i.e. precursors) which are transported to the vicinity of the substrate via the vapour phase. The film-forming chemical reactions typically utilize thermal energy from a heated substrate as depicted schematically in Figure 30. Other more special methods, which cannot be discussed here, couple non-thermal energy sources such as RF or microwave power or light into the reaction process in order to reduce the thermal reaction temperature required. In order to complete the system, a delivery system for the precursors and, finally, an exhaust system must be added. The most straightforward type of CVD involves chemical precursor compounds that are sufficiently stable gases and such processes are standard processes in CMOS technology for the deposition of insulators and interlayer dielectrics like poly-Si, SiO<sub>2</sub>, SiN<sub>x</sub> and BPSG glasses. Figure 31 shows the schematics of a reactor for handling large batches of wafers simultaneously. Examples of the reactions involved are the thermal decomposition of silane, SiH<sub>4</sub>, for the deposition of:

- Poly Si :  $\text{SiH}_4 \rightleftharpoons \text{Si(s)} + 2 \text{H}_2$  at 580-650 °C, and a pressure of  $\approx 1$  mbar;
- Si-Nitride:  $3 \text{SiH}_4 + 4 \text{NH}_3 \rightleftharpoons \text{Si}_3\text{N}_4 + 12 \text{H}_2$  at 700-900 °C, and atmospheric pressure;
- Si-Dioxide:  $\text{SiH}_4 + \text{O}_2 \rightleftharpoons \text{SiO}_2 + 2 \text{H}_2$  at 450 °C;

These SiO<sub>2</sub> films are usually under high stress and are not conformal. Therefore alternative routes using organic precursors have been developed e.g., the TEOS (tetra-ethyl-ortho-silane) process:



Similarly, for the processing of many metals and especially the group-II metals, special precursors in the form of organometallic compounds had to be developed and a special subgroup of CVD techniques, **metal-organic-CVD, MOCVD**, has therefore evolved. Efficient, reproducible MOCVD processes hinge critically upon precursors with high and stable vapour pressures and the chemistry is therefore the decisive step in the development of MOCVD.

**Main pros: suitable for VLSI, cheap, efficient, "conformal"**

**Main cons: purity (reaction products), relatively poor thickness and homogeneity control**

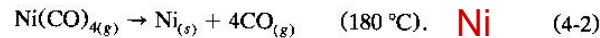
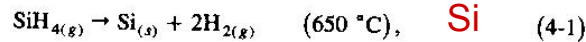
# Other CVD examples I

Da M. Ohring, The Materials Science of Thin Films, Academic (1992)

## A few common reactions for metals and semiconductors:

### 4.2.1. Pyrolysis

Pyrolysis involves the thermal decomposition of such gaseous species as hydrides, carbonyls, and organometallic compounds on hot substrates. Commercially important examples include the high-temperature pyrolysis of silane to produce polycrystalline or amorphous silicon films, and the low-temperature decomposition of nickel carbonyl to deposit nickel films.



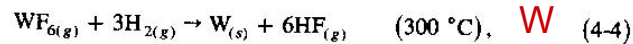
Interestingly, the latter reaction is the basis of the Mond process, which has been employed for over a century in the metallurgical refining of Ni.

### 4.2.2. Reduction

These reactions commonly employ hydrogen gas as the reducing agent to effect the reduction of such gaseous species as halides, carbonyl halides, oxyhalides, or other oxygen-containing compounds. An important example is the reduction of  $\text{SiCl}_4$  on single-crystal Si wafers to produce epitaxial Si films according to the reaction



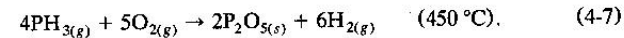
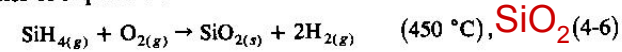
Refractory metal films such as W and Mo have been deposited by reducing the corresponding hexafluorides, e.g.,



Tungsten films deposited at low temperatures have been actively investigated as a potential replacement for aluminum contacts and interconnections in integrated circuits. Interestingly,  $\text{WF}_6$  gas reacts directly with exposed silicon surfaces, depositing thin W films while releasing the volatile  $\text{SiF}_4$  by-product. In this way silicon contact holes can be selectively filled with tungsten while leaving neighboring insulator surfaces uncoated.

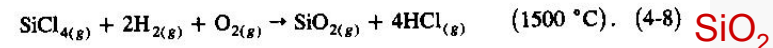
### 4.2.3. Oxidation

Two examples of important oxidation reactions are



The deposition of  $\text{SiO}_2$  by Eq. 4-6 is often carried out at a stage in the processing of integrated circuits where higher substrate temperatures cannot be tolerated. Frequently, about 7% phosphorous is simultaneously incorporated in the  $\text{SiO}_2$  film by the reaction of Eq. 4-7 in order to produce a glass film that flows readily to produce a planar insulating surface, i.e., "planarization."

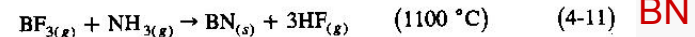
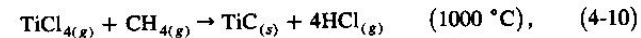
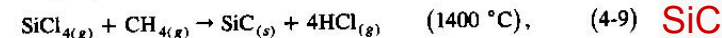
In another process of technological significance,  $\text{SiO}_2$  is also produced by the oxidation reaction



The eventual application here is the production of optical fiber for communications purposes. Rather than a thin film, the  $\text{SiO}_2$  forms a cotton-candy-like deposit consisting of soot particles less than  $1000 \text{ \AA}$  in size. These are then consolidated by elevated temperature sintering to produce a fully dense silica rod for subsequent drawing into fiber. Whether silica film deposition or soot formation occurs is governed by process variables favorable to heterogeneous or homogeneous nucleation, respectively. Homogeneous soot formation is essentially the result of a high  $\text{SiCl}_4$  concentration in the gas phase.

### 4.2.4. Compound Formation

A variety of carbide, nitride, boride, etc., films and coatings can be readily produced by CVD techniques. What is required is that the compound elements exist in a volatile form and be sufficiently reactive in the gas phase. Examples of commercially important reactions include

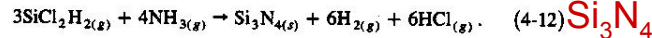


for the deposition of hard, wear-resistant surface coatings. Films and coatings of compounds can generally be produced through a variety of precursor gases and reactions. For example, in the much studied SiC system, layers were first

## Other CVD examples II

produced in 1909 through reaction of  $\text{SiCl}_4 + \text{C}_6\text{H}_6$  (Ref. 8). Subsequent reactant combinations over the years have included  $\text{SiCl}_4 + \text{C}_3\text{H}_8$ ,  $\text{SiBr}_4 + \text{C}_2\text{H}_4$ ,  $\text{SiCl}_4 + \text{C}_6\text{H}_{14}$ ,  $\text{SiHCl}_3 + \text{CCl}_4$ , and  $\text{SiCl}_4 + \text{C}_6\text{H}_5\text{CH}_3$ , to name a few, as well as volatile organic compounds containing both silicon and carbon in the same molecule (e.g.,  $\text{CH}_3\text{SiCl}_3$ ,  $\text{CH}_3\text{SiH}_3$ ,  $(\text{CH}_3)_2\text{SiCl}_2$ , etc.). Although the deposit is nominally SiC in all cases, resultant properties generally differ because of structural, compositional, and processing differences.

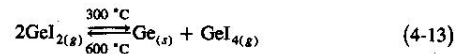
Impermeable insulating and passivating films of  $\text{Si}_3\text{N}_4$  that are used in integrated circuits can be deposited at  $750^\circ\text{C}$  by the reaction



The necessity to deposit silicon nitride films at lower temperatures has led to alternative processing involving the use of plasmas. Films can be deposited below  $300^\circ\text{C}$  with  $\text{SiH}_4$  and  $\text{NH}_3$  reactants, but considerable amounts of hydrogen are incorporated into the deposits.

### 4.2.5. Disproportionation

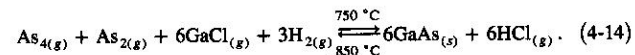
Disproportionation reactions are possible when a nonvolatile metal can form volatile compounds having different degrees of stability, depending on the temperature. This manifests itself in compounds, typically halides, where the metal exists in two valence states (e.g.,  $\text{GeI}_4$  and  $\text{GeI}_2$ ) such that the lower-valent state is more stable at higher temperatures. As a result, the metal can be transported into the vapor phase by reacting it with its volatile, higher-valent halide to produce the more stable lower-valent halide. The latter disproportionates at lower temperatures to produce a deposit of metal while regenerating the higher-valent halide. This complex sequence can be simply described by the reversible reaction



and realized in systems where provision is made for mass transport between hot and cold ends. Elements that have lent themselves to this type of transport reaction include aluminum, boron, gallium, indium, silicon, titanium, zirconium, beryllium, and chromium. Single-crystal films of Si and Ge were grown by disproportionation reactions in the early days of CVD experimentation on semiconductors employing reactors such as that shown in Fig. 4-2. The enormous progress made in this area is revealed here.

### 4.2.6. Reversible Transfer

Chemical transfer or transport processes are characterized by a reversal in the reaction equilibrium at source and deposition regions maintained at different temperatures within a single reactor. An important example is the deposition of single-crystal (epitaxial) GaAs films by the chloride process according to the reaction



Here  $\text{AsCl}_3$  gas from a bubbler transports Ga toward the substrates in the form of  $\text{GaCl}$  vapor. Subsequent reaction with  $\text{As}_4$  causes deposition of GaAs.

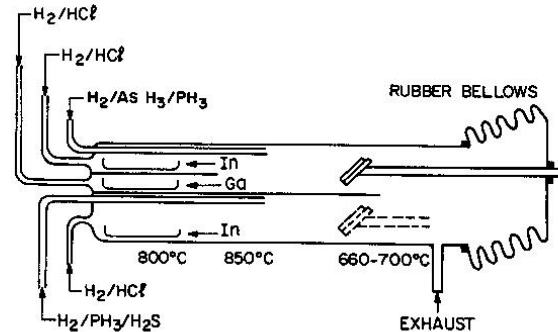
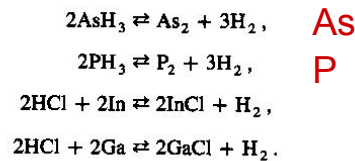
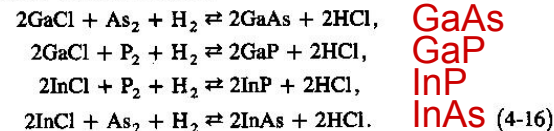


Figure 4-3. Schematic of atmospheric CVD reactor used to grow GaAs and other compound semiconductor films by the hydride process. (Reprinted with permission from Ref. 10).

Alternatively, in the hydride process, As is introduced in the form of  $\text{AsH}_3$  (arsine), and  $\text{HCl}$  serves to transport Ga. Both processes essentially involve the same gas-phase reactions and are carried out in similar reactors, shown schematically in Fig. 4-3. What is significant is that single-crystal, *binary* (primarily GaAs and InP but also GaP and InAs) as well as *ternary* (e.g.,  $(\text{Ga}, \text{In})\text{As}$  and  $\text{Ga}(\text{As}, \text{P})$ ) compound films have been grown by these vapor phase epitaxy (VPE) processes. Similarly, in addition to binary and ternary semiconductor films, *quaternary* epitaxial films containing controlled amounts of Ga, In, As, and P have been deposited by the hydride VPE process. Combinations of gas mixtures and more complex reactors are required in this case to achieve the desired stoichiometries. The resulting films are the object of intense current research and development activity in a variety of optoelectronic devices (e.g., lasers and detectors). For quaternary alloy deposition by the hydride process, single-crystal InP substrates are employed. Gas-phase source reactions include



Deposition reactions at substrates include



**Reactivity enhancement can be achieved by several methods, e.g., formation of a plasma (see Plasma-Enhanced CVD for CNT fabrication!)**

Da M. Ohring, The Materials Science of Thin Films, Academic (1992)

# CVD and MO-CVD

## 4.1.1 Precursor Chemistry and Delivery

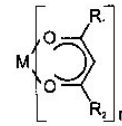
Only a sufficiently high vapour pressure enables vapour-phase mixing of precursor components and transport of the reactants to the growing film and a vapour pressure of  $> 0.1$  mbar at  $100^\circ\text{C}$  is considered to be a lower limit. Adequate molecular stability of the precursor vapour is required to prevent premature reaction or decomposition of the precursor during vapour phase transport; these requirements characterize a process window between vaporization and decomposition of the precursor. Additional requirements are long-term stability of the precursors (e.g. low moisture sensitivity), complete decomposition (no contamination of the film e.g. by fluorine) and last but not least low toxicity and environmental regulatory requirements.

For complex oxides the precursor molecules typically contain the metal atoms, M, and organic groups, R. In most cases, such as in alkoxides, ketonates, and carboxylates, the metal atom is bound to the organic group through an oxygen atom, i.e. M-O-R. This is different from precursors used for the MOCVD of compound semiconductors where the precursors are conventional metal organic compounds, i. e. M-R systems. For heavy cations (especially group-II elements), a reasonable volatility is often reached only by organometallic precursors, e.g. by  $\beta$ -diketonates with several alkyl groups, such as in tetramethylheptadionates (thd) (and this type of organometallic precursor is the origin of an alternative acronym occasionally used: OMCVD). The two keto groups chelate the cation while the outer alkyl groups effectively shield any polar region of the molecule. Typically two (thd) ligands are reacted with one cation yielding  $\text{Ba}(\text{thd})_2$ . Since the outer shell of this molecule consists entirely of alkyl groups there is only a weak van-der-Waals interaction between neighbouring molecules and, hence, a relatively low boiling temperature. For cations with a higher electronegativity (i.e. a lower tendency to form ionic bonds), alkyl compounds, such as  $\text{Pb}(\text{C}_2\text{H}_5)_4$ , and alkoxide compounds, such as  $\text{Ti}(\text{OC}_3\text{H}_7)_4$ , may give rise to a sufficient volatility [23].

The different types of precursors used for oxide deposition are summarized in Figure 32. The main applications for the present topics of IT are included in the figure: e.g., the diketonates for Ba and Sr, thd = tetramethylheptadionate, alkoxides for Ti (TIP = titaniumisopropoxide =  $\text{Ti}(\text{O-i-Pr})_4$ ) and Zr. Mixed precursors like  $\text{Ti}(\text{O-i-Pr})_2(\text{thd})_2$  are also used to increase compatibility with other precursors. In addition, adducts or stabilizers are used in order to avoid reactions and oligomerization e.g., tetraglyme or pmdeta. Most of these precursors are liquid or solid at room temperature and reach a sufficient vapour pressure only at elevated temperature. Therefore, special delivery systems are necessary, i.e. bubblers or liquid source delivery systems.

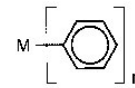
**Chemical Vapor methods do strongly rely on the availability of suitable precursors, i.e., compounds able to efficiently react with the environment gas and deposit onto the substrate**

### $\beta$ -Diketonates

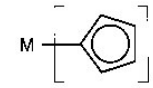


- $\text{R}_1=\text{R}_2=\text{CH}_3$  (acetylacetonate)
- $\text{R}_1=\text{R}_2=\text{C}(\text{CH}_3)_2$  (tetramethylheptadionate) ..... **Ba(thd)<sub>2</sub>, Sr(thd)<sub>2</sub>**
- $\text{R}_1=\text{C}(\text{CH}_3)_2, \text{R}_2=\text{CF}_3$  (trifluorodimethylhexanedionate)
- $\text{R}_1=\text{C}(\text{CH}_3)_2, \text{R}_2=\text{C}_2\text{F}_5$  (heptafluorodimethyloctanedionate)
- $\text{R}_1=\text{R}_2=\text{CF}_3$  (hexafluoroacetylacetonate)

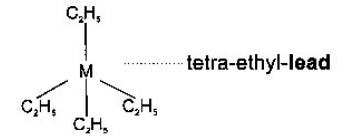
### Organometallics



phenyl



cyclopentadienide

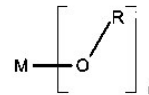


tetra-ethyl-lead

tetraethyl

triphenyl-Bi

### Alkoxides



- $\text{R}=\text{CH}_3$  (methoxide)
- $\text{R}=\text{C}_2\text{H}_5$  (ethoxide)
- $\text{R}=\text{CH}(\text{CH}_3)_2$  (isopropoxide) ..... **Ti: TIP, Zr: ZIP**
- $\text{R}=\text{C}(\text{CH}_3)_3$  (t-butoxide) ..... **Zr -tert -butoxide**

**Figure 32:** Selection of precursor molecules for oxide deposition [25].

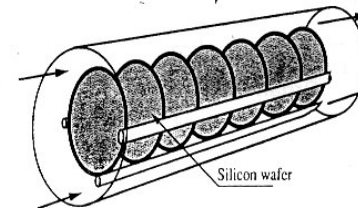
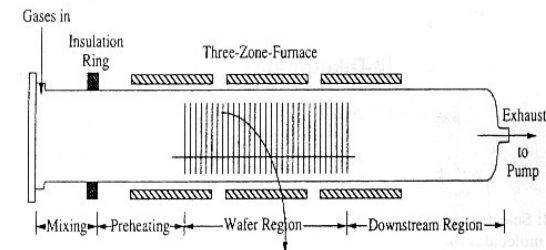


**Figure 31:** Schematic representation of a hot-wall multiple-wafer in-tube CVD reactor [20].

## 4.B. Examples of deposition from the liquid phase (CSD)

### 4.2 Chemical Solution Deposition

The chemical solution deposition (CSD) method comprises a range of deposition techniques and of chemical routes which have been reviewed recently [23], [33]. A generalized flow chart of the CSD of oxide thin films is shown in Figure 42. The process starts with the preparation of a suitable coating solution from precursors according to the designated film composition and the chemical route to be used. Besides mixing, preparation may include the addition of stabilizers, partial hydrolysis, refluxing, or else. The coating solution is then deposited onto substrates by:

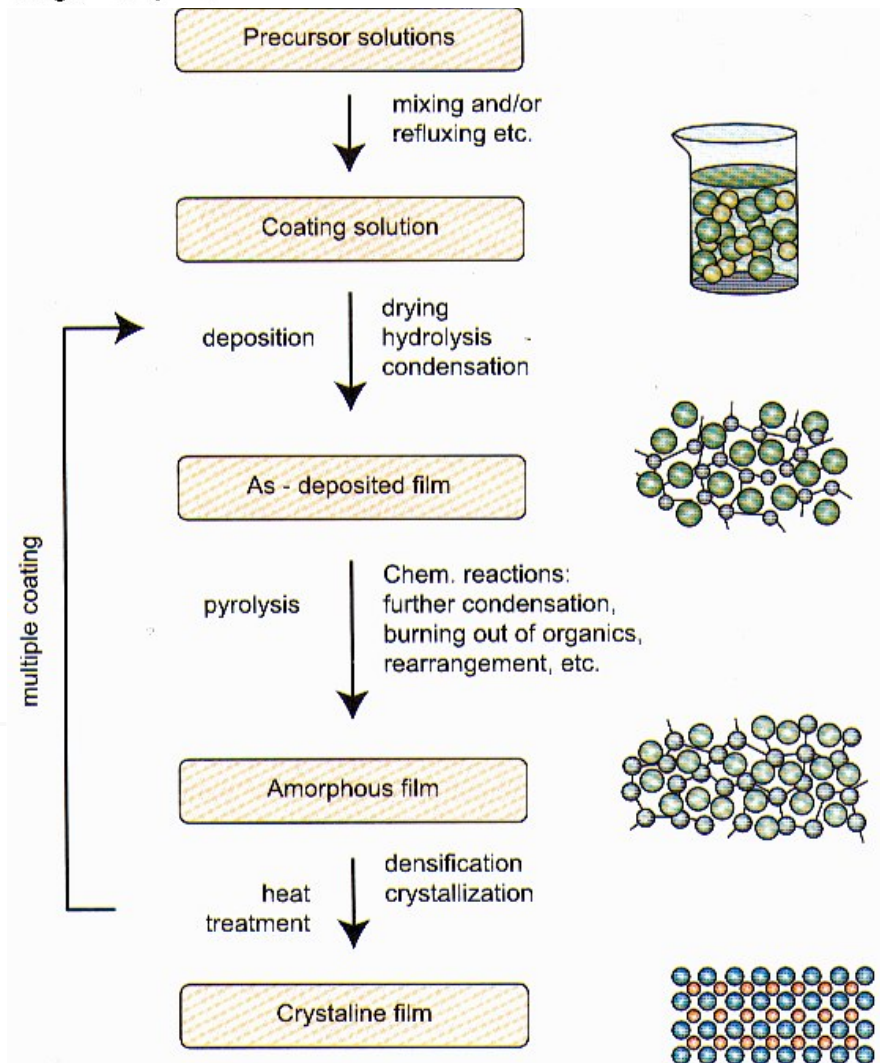
- *spin-coating*, where typically a photoresist spinner is employed and which is suitable for semiconductor wafers,
- *dip coating*, which is often used in the optics industry for large or non-planar substrates, and
- *spray coating*, which is based on a misting of the coating solution and deposition of the mist exploiting gravitation or an electrostatic force.

The wet film may undergo drying, hydrolysis and condensation reactions depending on the chemical route. The as-deposited film possibly represents a chemical or physical network. Upon subsequent heat treatment, a further hydrolysis and condensation and/or a pyrolysis of organic ligands may take place, again depending on the chemical route. The resulting film consists of amorphous or nanocrystalline oxides and/or carbonates. Upon further heat treatment, any carbonate will decompose and the film will crystallize through a homogeneous or a heterogeneous nucleation. Typically, the desired final film thickness is built up by multiple coating and annealing.

Depending on the type and reactivity of the precursors, the chemistry shows a wide spectrum of reaction types. On the one hand, there are the pure sol-gel reactions i.e. alkoxide precursor systems, which undergo hydrolysis and condensation reactions. The formation of  $\text{SiO}_2$  coatings starting from Si alkoxides is the classical example of this type of reaction. The condensation leads to a chemical gelation in which – under appropriate reaction conditions – no pyrolysis reaction of any organic ligand occurs. At the other extreme, there is metal organic decomposition (MOD), which typically starts from carboxylates of the cations or, in special cases, from the nitrates. The carboxylates do not chemically react with water. Consequently, during heat treatment, first the solvents are evaporated, a process which is sometimes referred to as physical gelation. Upon further heating, the carboxylates pyrolytically decompose into amorphous or nanocrystalline oxides or carbonates. There is a wide spectrum of possible reaction routes between the pure sol-gel route and the MOD route. Depending on the type of alkoxides and a possible stabilization of the precursors, there may be a partial hydrolysis and condensation while some organic ligands remain in the gelled film and undergo pyrolysis upon further heat treatment. In the synthesis of multicomponent oxide films, often hybrid routes are followed, i.e. there may be some precursors employed which tend to follow the sol-gel or partial sol-gel route while others undergo typical MOD reactions.

The microstructure formed during the CSD process strongly depends on the thermodynamics and kinetics of the solidstate reaction from the intermediate amorphous or nanocrystalline state after pyrolysis to the final equilibrium crystalline phase. This is controlled by the chemical composition of the film system (for details see e.g. ref. [23]).

Due to their low capital investment and simple processing, CSD techniques are widely used and are also applicable for micro- and nanoelectronics on a low level of integration, e.g. for present state FeRAMs.

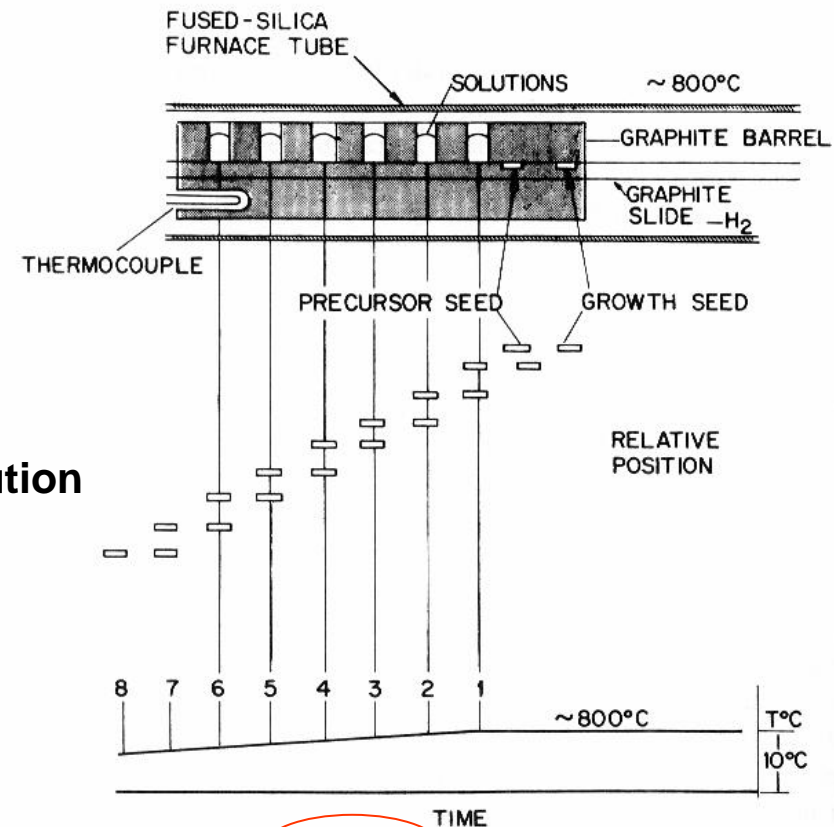


# Liquid Phase Epitaxy (LPE) and Sol-Gel

Da M. Ohring, The Materials Science of Thin Films, Academic (1992)

## LPE: deposition from a super-saturated solution

techniques. LPE involves the precipitation of a crystalline film from a super-saturated melt onto the parent substrate, which serves as both the template for epitaxy and the physical support for the heterostructure. The process can be understood by referring to the GaAs binary-phase diagram on p. 31. Consider a Ga-rich melt containing 10 at% As. When heated above 950°C, all of the As dissolves. If the melt is cooled below the liquidus temperature into the two-phase field, it becomes supersaturated with respect to As. Only a melt of lower than the original As content can now be in equilibrium with GaAs. The excess As is, therefore, rejected from solution in the form of GaAs that grows epitaxially on a suitably placed substrate. Many readers will appreciate that the



## Sol-Gel: deposition from precursors in a gel solution

Some **advantages** of chemical methods:

- Cheapness;
- Scalability;
- Growth rate

Main **disadvantages**:

- Poor control of the film homogeneity;
- Limited applicability (precursors are frequently needed!);
- Need of several process steps and integrability issues

Figure 7-17. Schematic of LPE reactor. (Courtesy of M. B. Panish, AT&T Bell Laboratories.)

## Conclusions

- ✓ Thin films are an essential component for any nanotechnology application (not only, but especially, electronics)
- ✓ Many deposition methods have been developed and applied
- ✓ Film growth typically involves arrival of elemental materials onto a substrate (and subsequent surface processes, like diffusion, nucleation and coalescence): *physical* and *chemical* techniques can be used to produce the elemental materials from a solid or gaseous (or liquid) material
- ✓ Every technique holds specific advantages and limitations: no “universal” method exists